MCDONNELL DOUGLAS ASTRONAUTICS COMPANY

MCDONNELL DOUGLAS CORPORATION

30-2214-02 (08 JAN 70)

MCDONNELL DOUGLAS CORPORATION

STATISTICAL ENERGY ANALYSIS OF COMPLEX STRUCTURES PHASE II

Final Report

September 1980

MDC G9203

Prepared by

R. W. Trudell
L. I. Yano

Approved by:

R. F. Zemer
Director - Structures & Materials
Engineering Division

MCDONNELL DOUGLAS ASTRONAUTICS COMPANY-HUNTINGTON BEACH

5301 Bolsa Avenue Huntington Beach, California 92647 (714) 896-3311

PREFACE

This document is submitted by the McDonnell Douglas Astronautics Company to the National Aeronautics and Space Administration and was prepared under Contract NAS8-33191, "Statistical Energy Analysis of Complex Structures (Phase 2)." The study was directed by R. W. Trudell. W. Clever of the Vibration Analysis Branch, Systems Dynamics Laboratory, Marshall Space Flight Center, administered and directed the contract.

CONTENTS

FIGURES

TABLES

SYMBOLS

A	area
A_s	surface area of element exposed to acoustic excitation
C_o	speed of sound in air
C_g	group velocity $= 1.07[\omega C_\ell t]^{\frac{1}{2}}$
C_ℓ	longitudinal wave velocity
D	plate bending rigidity $= \frac{Eh^3}{12(1-\nu^2)}$
E	modulus of elasticity, total energy of element
L	joint length
N	number of modes
S	power input
a	acceleration
f	frequency
f_r	ring frequency
g	gravitational acceleration
h_i	plate thickness
k_p	radius of gyration of plate
ℓ	length
m	mass
n	modal density
p	pressure
r	radius
t	thickness

v	velocity
$\bar{w}$	weight density
α	SEA response equation coefficient
Δ	increment
η	element loss factor
γ	Poisson's ratio
π	3.14159
ρ	mass density
σ	radiation efficiency
τ	joint loss coupling parameter
ϕ_{ij}	power transfer coefficient for coupling between modes in elements i and j
ω	frequency in radians/second, normally center frequency of a frequency band

NOTATION

Element	a set of modes modeled as one unit of a system
System	the total structure and associated energy sources under consideration
$\langle\!\!\langle \quad \rangle\!\!\rangle$	indicates averaging over both time and space

Section 1
INTRODUCTION

Statistical Energy Analysis (SEA) is a method of estimating the structural vibration properties of complex systems in high frequency environments. The method considers the average distribution and transfer of energy among the modes of a vibrating system and assumes that all of the vibratory energy of the system is contained in these modes. The analysis method generally involves averaging structural responses over time and space.

The response predictions are made by modeling the structure into relatively gross elements, deriving power flow equations between these elements and the environment, and solving the resulting system of equations for element response levels.

The general assumptions which SEA is based on are:

1) The total vibrating system can be partitioned into SEA elements (with suitable boundary conditions) whose modes approximate the modes of the original vibrating system.

2) The modes of the elements of a system contain all of the vibratory energy of the system.

3) Only modes occurring within the same frequency band are coupled.

4) The energy in one frequency band of a system element is equally distributed among the modes of that element occurring in the frequency band.

5) For two coupled elements, all of the modes occurring in one of the elements in one frequency band are equally coupled to each mode occurring in the same frequency band in the other element.

A more thorough treatment of SEA is contained in the references.

Section 2

VIBRATION PREDICTION FOR PAYLOAD/SUPPORT STRUCTURE WITH ACOUSTIC EXCITATION

The structure analyzed was the Materials Experiment Assembly (MEA) (Figure 1), a portion of the OSTA-2 payload for the Space Transportation System. SEA techniques were used to model the structure and predict structural element responses to given acoustic excitation. The predicted responses were compared with the physical test results obtained at MSFC for evaluation of SEA accuracy.

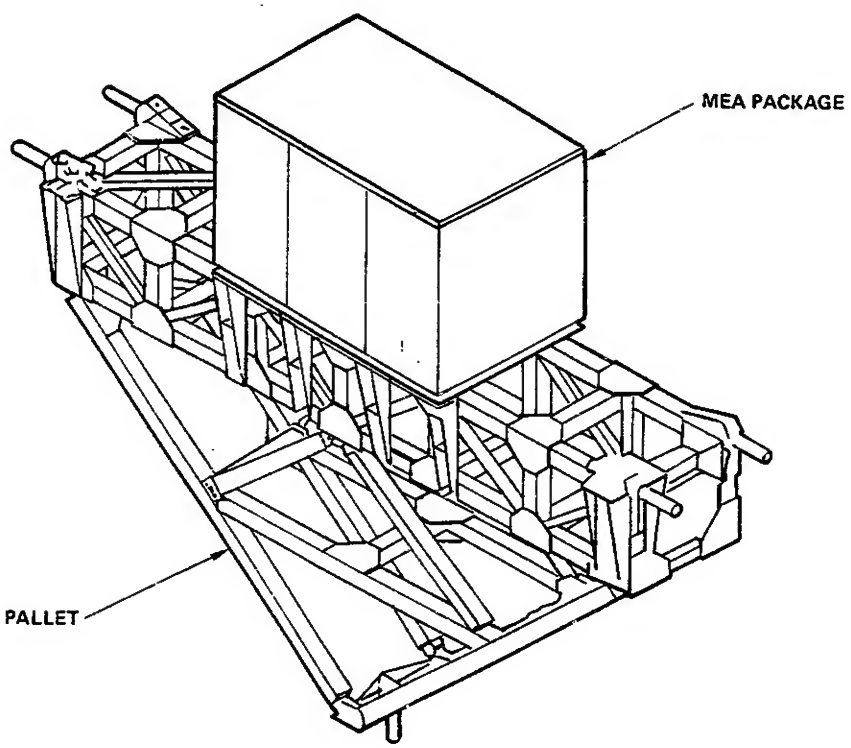

Figure 1. OSTA-2 Aft MEA MPE Support Structure

2.1 MODELING

The structure was represented by six SEA elements chosen, to the maximum practical extent, to correspond with MEA acoustic test accelerometer locations. This was done to assure valid comparisons between the response predictions and the corresponding acoustic test data. A schematic of the MEA model is shown in Figure 2, and the structural element breakdown, numbering scheme, and connectivity are shown in Figure 3.

The general SEA response equations for the six-element system with external excitation are:

$$\begin{vmatrix} \alpha_{11} & \alpha_{12} & \alpha_{13} & \alpha_{14} & \alpha_{15} & \alpha_{16} \\ & \alpha_{22} & \alpha_{23} & \alpha_{24} & \alpha_{25} & \alpha_{26} \\ & & \alpha_{33} & \alpha_{34} & \alpha_{35} & \alpha_{36} \\ & & & \alpha_{44} & \alpha_{45} & \alpha_{46} \\ \text{SYMMETRIC} & & & & \alpha_{55} & \alpha_{56} \\ & & & & & \alpha_{66} \end{vmatrix} \cdot \begin{Bmatrix} E_1 \\ E_2 \\ E_3 \\ E_4 \\ E_5 \\ E_6 \end{Bmatrix} = \begin{Bmatrix} S_1 \\ S_2 \\ S_3 \\ S_4 \\ S_5 \\ S_6 \end{Bmatrix}$$

$$\alpha_{ij} = \begin{cases} -N_i\phi_{ij} & i \neq j \\ \omega\eta_j + \sum_{k=1}^{6} N_k\phi_{ik} & i = j \end{cases}$$

N_i = number of modes resonant in element i

η_i = element i loss factor

ϕ_{ij} = power transfer coefficient for coupling between modes in elements i and j

ω = center frequency of bandwidth

$E_i = m_i \frac{\overline{\langle a_i^2 \rangle}}{\omega^2}$ = total energy of element i

S_i = external acoustic or mechanical excitation in the bandwidth of interest

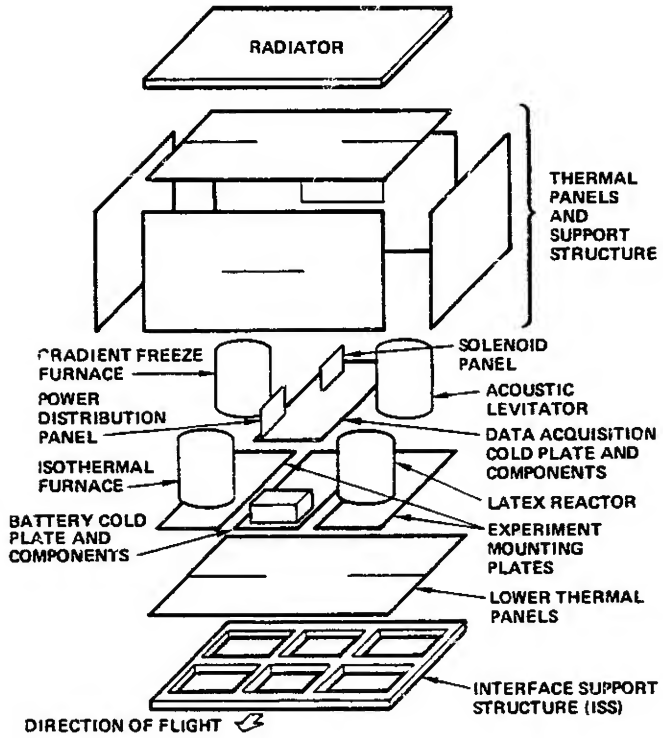

Figure 2. Material Experiments Assembly (MEA) Structural Breakdown (some components and details omitted)

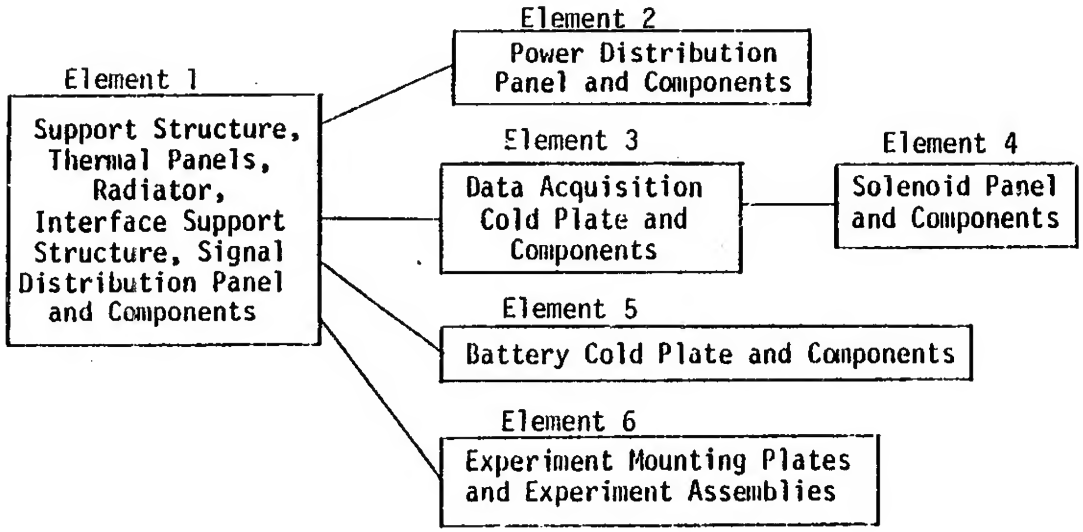

Figure 3. SEA Model Elements for Acoustic Test Configuration

Since all of the elements are not physically connected to each other, the coefficient for power transfer between elements (ϕ_{ij}) can be set to zero. This reduces the system of equations to:

$$\begin{vmatrix} \alpha_{11} & \alpha_{12} & \alpha_{13} & & \alpha_{15} & \alpha_{16} \\ \alpha_{21} & \alpha_{22} & & & & \\ \alpha_{31} & & \alpha_{33} & \alpha_{34} & & \\ & & \alpha_{43} & \alpha_{44} & & \\ \alpha_{51} & & & & \alpha_{55} & \\ \alpha_{61} & & & & & \alpha_{66} \end{vmatrix} \begin{vmatrix} E_1 \\ E_2 \\ E_3 \\ E_4 \\ E_5 \\ E_6 \end{vmatrix} = \begin{vmatrix} S_1 \\ 0 \\ 0 \\ 0 \\ 0 \\ 0 \end{vmatrix}$$

2.2 DAMPING

A loss factor of $\eta = 0.01$ was used for all other elements, based on $Q = 100$ being a reasonable value for aluminum plates. The loss factor includes the contributions of internal energy losses, joint dissipations not included in the coupling loss factor, and losses due to radiation.

2.3 MODAL DENSITY

The number of modes (N_i) used in the response equations is determined by:

$$N_i = n_i(\Delta f)$$

where n_i = modal density of element i

Δf = bandwidth of the analysis.

Element 1 of the MEA structure consists of the package support structure, thermal panels, radiator, interface support structure (ISS), and the signal distribution panel and components. The element modal density was calculated by summing the modal density contributions of the element substructure. Since the thermal panels consist of fiberglass plates separated by insulating material, there is assumed to be no mechanical coupling between the

inner and outer plates (Reference 1). Therefore, they were modeled as two equivalent aluminum plates acting independently. The thermal panels were redefined as equivalent aluminum panels based on the respective material stiffness properties to aid in the ease of computations. All other parts are plates or are formed by multiple plate sections. Therefore, using the approximate equation for the high frequency modal density of plates, the element modal density could be found as:

$$n_1(f) = \sum \frac{A}{2 k_p C_\ell}$$

$$= \frac{1}{2\sqrt{\frac{Eg}{12\overline{w}(1-\nu^2)}}} \sum \frac{A}{t}$$

where A = surface area of plate

t = thickness of plate

$\overline{w}$ = weight density of plate (0.101 lb/in^3 for aluminum)

E = modulus of elasticity

G = 386 in./s^2

ν = Poisson's ratio

$n_1(f)$ = 6.30 modes/Hz

Elements 2, 3, 4 and 5 consist of panels that are loaded by various components. Sevy and Earls (Reference 2) indicate that loaded panels will exhibit a greater stiffness and lower modal density than an identical unloaded panel. An increase in stiffness by a factor of 2 gave reasonable results in work done by Davis (Reference 3), and was assumed to apply for these elements. The resulting modal density for these elements could be found by the relationship

$$n_i(f) = \frac{1}{2\sqrt{\frac{Eg}{12\bar{w}(1-\nu^2)}}} \frac{1}{\sqrt{2}} \frac{A}{t}$$

$n_2(f) = .0110$ mode/Hz

$n_3(f) = .0076$ mode/Hz

$n_4(f) = .0237$ mode/Hz

$n_5(f) = .0083$ mode/Hz

Element 6 consists of the experiment mounting plates and the experiment assemblies. The modal density of the experiment mounting plates can be determined as for element 1. The experiment assembly is made up of a cylinder capped by a dome. The approximate modal density of a cylinder is found by:

$$n_6(f) = \frac{A_S}{2 k_p C_\ell} \qquad \text{for } \frac{f}{f_r} > 1$$

$$= \frac{A_S}{2 k_p C_\ell} \left(\frac{f}{f_r}\right)^{2/3} \qquad \text{for } \frac{f}{f_r} < 1$$

Substituting for $k_p(C_\ell)$ as in the equation for element 1, the modal density for element 6 is expressed as

$$n_6(f) = \frac{A_S}{2\sqrt{\frac{Eg}{12\bar{w}(1-\nu^2)}}} \qquad \frac{f}{f_r} > 1$$

$$= \frac{A_S}{2\sqrt{\frac{Eg}{12\bar{w}(1-\nu^2)}}} \left(\frac{f}{f_r}\right)^{2/3} \qquad \frac{f}{f_r} < 1$$

where f_r = ring frequency of a cylinder (the frequency whose wavelength equals the cylinder circumference) = $\frac{1}{2\pi r}\sqrt{\frac{E}{\rho}}$

The equation for the modal density of a doubly curved surface (Reference 4)

is an expression that is not readily evaluated, so the modal density of the experiment housing cap was approximated using the relation for a flat plate:

$$n_6(f) = n_{plate} + n_{cylinder} + n_{cap} \quad \text{for each experiment assembly.}$$

$$n_6(f) = 0.609 \text{ mode/Hz} \qquad \frac{f}{f_r} > 1$$

$$= \left[0.444 \left(\frac{f}{f_r}\right)^{2/3} + 0.164\right] \text{ modes/Hz} \qquad \frac{f}{f_r} < 1$$

where $f_r = 3660$ Hz.

2.4 STRUCTURAL COUPLING

All of the joints between elements are essentially plates joined at right angles. The relation for modal coupling for this type of joint is:

$$\phi_{ij} = \frac{\omega}{N_j} \frac{C_{gL}}{2\pi^2 f A_i} \tau$$

for: Plate i | Plate j

$$C_g = 1.07\sqrt{\omega C_\ell t}$$

$$C_\ell = \sqrt{\frac{Eg}{\overline{w}(1-\nu^2)}}$$

L = joint length

$$\tau = \frac{8}{27} \qquad D_i \simeq D_j$$

$$= \frac{h_i}{h_j} \qquad D_i << D_j$$

where D = plate rigidity $= \frac{Eh^3}{12(1-\nu^2)}$

h_i = thickness of plate i

$h_i < \frac{h_j}{2}$ is the condition for $D_i \ll D_j$

i, j denote the elements that are coupled

The element coupling coefficients calculated using this relationship are

$$\phi_{12} = \frac{0.52}{\sqrt{f}}$$

$$\phi_{13} = \frac{1.26}{\sqrt{f}}$$

$$\phi_{15} = \frac{1.00}{\sqrt{f}}$$

$$\phi_{16} = \frac{0.29}{\sqrt{f}} \qquad \frac{f}{f_r} > 1$$

$$= \frac{0.18}{.00187f^{7/6} + .164\sqrt{f}} \qquad \frac{f}{f_r} < 1$$

$$\phi_{34} = \frac{38.6}{\sqrt{f}}$$

where $\phi_{ij} = \phi_{ji}$

2.5 ELEMENT ENERGY

The energy of the model elements is represented by

$$E_i = m_i \overline{\langle v_i^2 \rangle}$$

$$= m_i \frac{\overline{\langle a_i^2 \rangle}}{\omega^2}$$

where $\overline{<\ >}$ indicates averaging over time and space

m_i = mass of element i obtained from MEA weight status summary

m_1 = 615.14/g

m_2 = 28.0/g

m_3 = 108.84/g

m_4 = 26.54/g

m_5 = 670.0/g

m_6 = 567.28/g

2.6 ACOUSTIC POWER INPUT

The external acoustic field is assumed to be reverberant, therefore the power input term can be represented by

$$S_1 = \frac{2\pi^2 C_0^2 A_1 \overline{<P^2>} \sigma N_1(\text{surface})}{\omega^2(\Delta\omega)\, m_1}$$

The surfaces of the MEA package directly excited by the acoustic field were assumed to be comprised of the thermal panels, the radiator, and the interface support structure. The modal densities of these parts were found using the following relationships:

$$n(f) = \frac{A_S}{2 k_p C_\ell} = \frac{A_S}{2t\sqrt{\dfrac{Eg}{12\overline{w}(1-\nu^2)}}}$$

$$m = \overline{w} A_S\, t/g$$

$$N = n(f)\, \Delta f$$

It can be shown that

$$\left(\frac{A_1 N_1}{m_1}\right)_{\text{surface}} = \frac{\Delta f}{2}\sqrt{\frac{12g(1-\nu^2)}{\overline{w}E}}\left[\left(\frac{A}{t^2}\right)_{\text{panels}} + \left(\frac{A}{t^2}\right)_{\text{radiator}} + \left(\frac{A}{t^2}\right)_{\text{ISS}}\right]$$

The thermal panels are made up of insulating material sandwiched between fiberglass cover panels. When two plates are separated by an air space or by loose filler materials (which is the case here), no mechanical coupling between the plates can be assumed. However, there is acoustic coupling, so the inner and outer panels were assumed to act independently with a resultant doubling of the thermal panel contributory surface area. Equivalent aluminum panels were calculated based on the ratio of the modulus of elasticity of aluminum to the modulus of the panel material.

Therefore,

$$\left(\frac{A_1 N_1}{m_1}\right)_{\text{surface}} = 7.412 \times 10^5 \, \Delta f$$

The acoustic level criteria used in qualification testing of the MEA package are shown in Figure 4 and listed in Table 1. The values for each 1/3 octave band center frequency were used as the acoustic pressure input where

$$\langle p^2 \rangle = 10^{spl/10}(8.41 \times 10^{-18})$$

Radiation efficiency values were obtained from Figure 5, based on a coincidence frequency F_c = 10,400 Hz (for an equivalent aluminum panel thickness t_{eq} = 0.0368 in.). These values are also listed in Table 1. The input term is therefore

$$S_1 = \frac{C_0^2 \, 10^{spl/10}(8.41 \times 10^{-18}) \, \sigma(7.412 \times 10^5 \Delta f)}{4\pi f^2}$$

where C_0 = speed of sound in air
= 13,400 in./s at 15°C, 60°F

Table 1

SOUND PRESSURE LEVELS AND RADIATION EFFICIENCY
FOR USE IN SEA

FREQ.	SPL (dB)	RADIATION EFFICIENCY σ
31.5	120.0	.0191
40	122.0	.0191
50	124.0	.0191
63	126.0	.0191
80	128.0	.0191
100	130.0	.0191
125	132.0	.0191
160	133.0	.0191
200	134.5	.0191
250	135.0	.0191
320	135.0	.0191
400	135.0	.0200
500	135.0	.0209
630	133.0	.0224
800	131.0	.0240
1000	127.0	.0251
1250	126.0	.0275
1600	125.0	.0302
2000	123.0	.0355
2500	121.0	.0417
3150	119.0	.0501
4000	117.0	.0708
5000	115.0	.1059

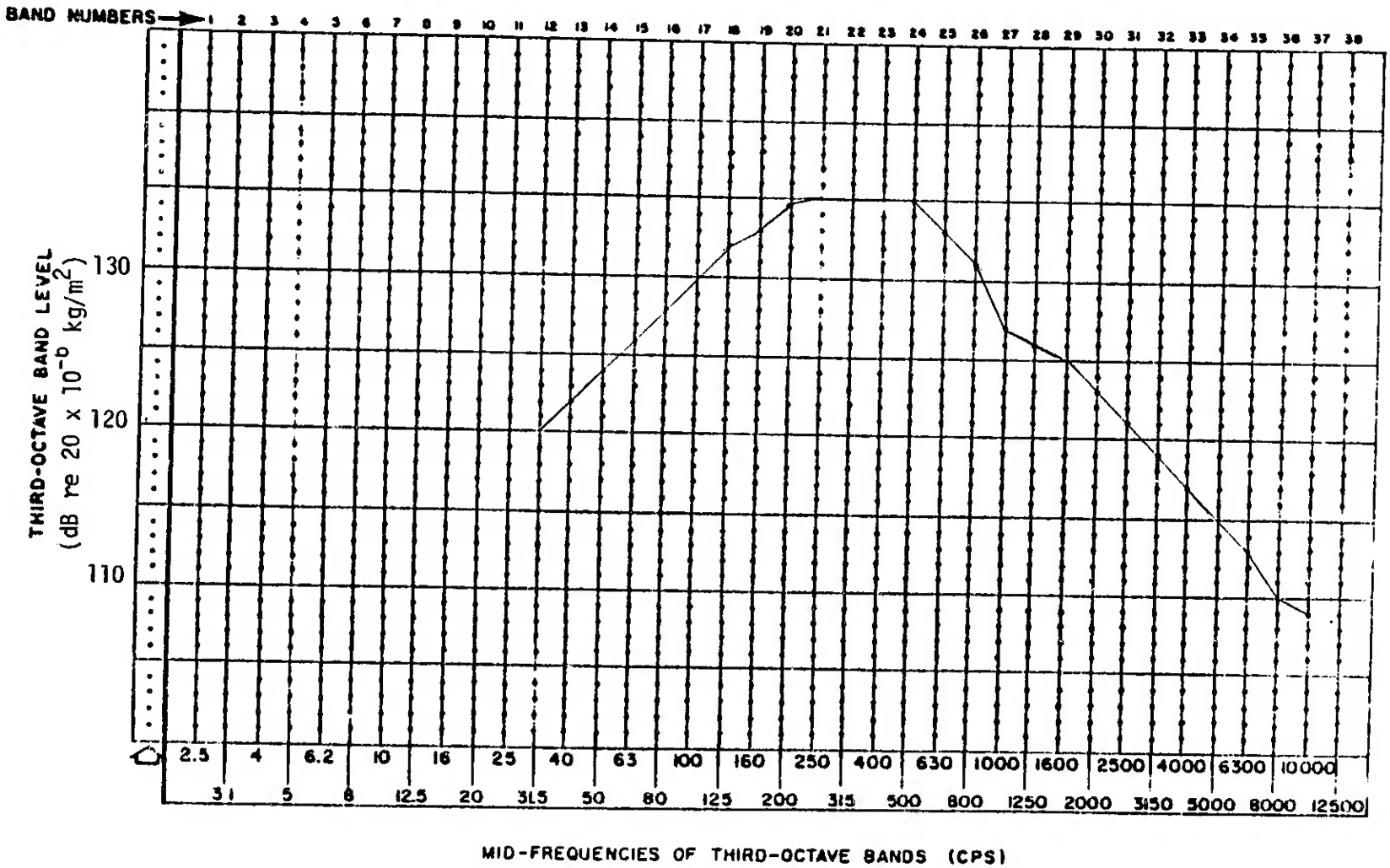

Figure 4 - One-Third Octave Band Acoustic Specification

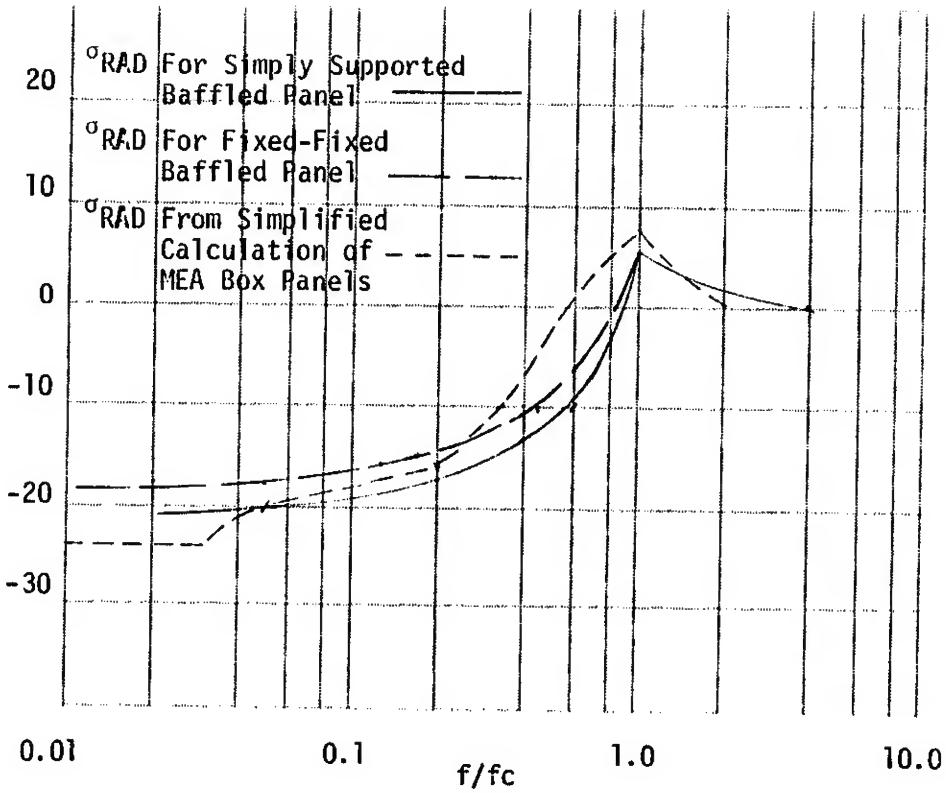

Figure 5 - Radiation Efficiency of a Panel

2.7 INITIAL RESPONSE SOLUTION

The response predictions for the elements were determined in each 1/3 octave bandwidth from 31.5 to 5000 Hz by solving the system of equations for $\langle \bar{a}_i^2 \rangle$. The acceleration spectral density levels were then found where

$$PSD(f)_i = \frac{\langle \bar{a}_i^2 \rangle}{g^2 \Delta f}$$

The root-mean-squared accelerations in the 1/3 octave band could be calculated from the relationship

$$(g_{rms})_i = \sqrt{\frac{\langle \bar{a}_i^2 \rangle}{g^2}}$$

2.8 COMPARISON OF INITIAL RESPONSE PREDICTIONS AND MEASURED ACOUSTIC TEST DATA

Comparisons between the SEA vibration response predictions and acoustic test data provided by MSFC were made by comparing plots of acceleration PSD's calculated for each structural element against plots of acceleration PSD's for measurements normal to the surface of the respective element.

The acoustic test data consisted of 10 Hz bandwidth PSD measurements. In order to obtain a more appropriate comparison with the proper smoothing at higher frequencies, 1/3 octave band PSD's were formally computed from the 10 Hz bandwidth acoustic test data. The comparisons between the SEA predictions and all applicable test measurements are shown in Figures 6-11. The locations and orientations of the measurement points are identified in Table 2 and Figure 12.

The predicted response levels for element 1 show very good correlation with measurements 24X and 25Y (Figure 6), except at low frequencies. Test points 24X and 25Y both measure accelerations normal to the surface of the structure, which is consistent with the direction of SEA predictions. The overprediction of SEA at lower frequencies can be related to the

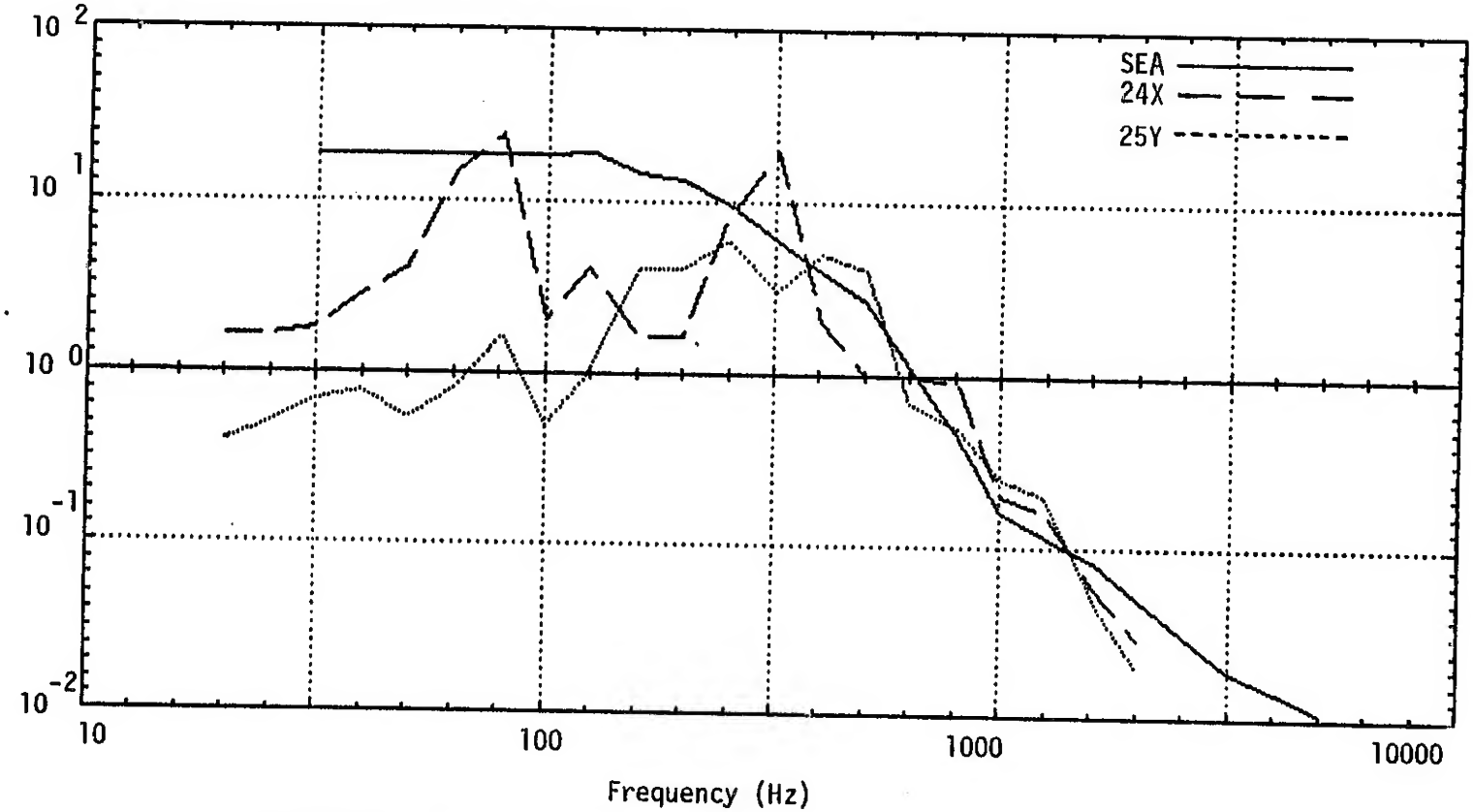

Figure 6 - Comparison of Initial SEA Prediction and Acoustic Test Measurements for Element 1

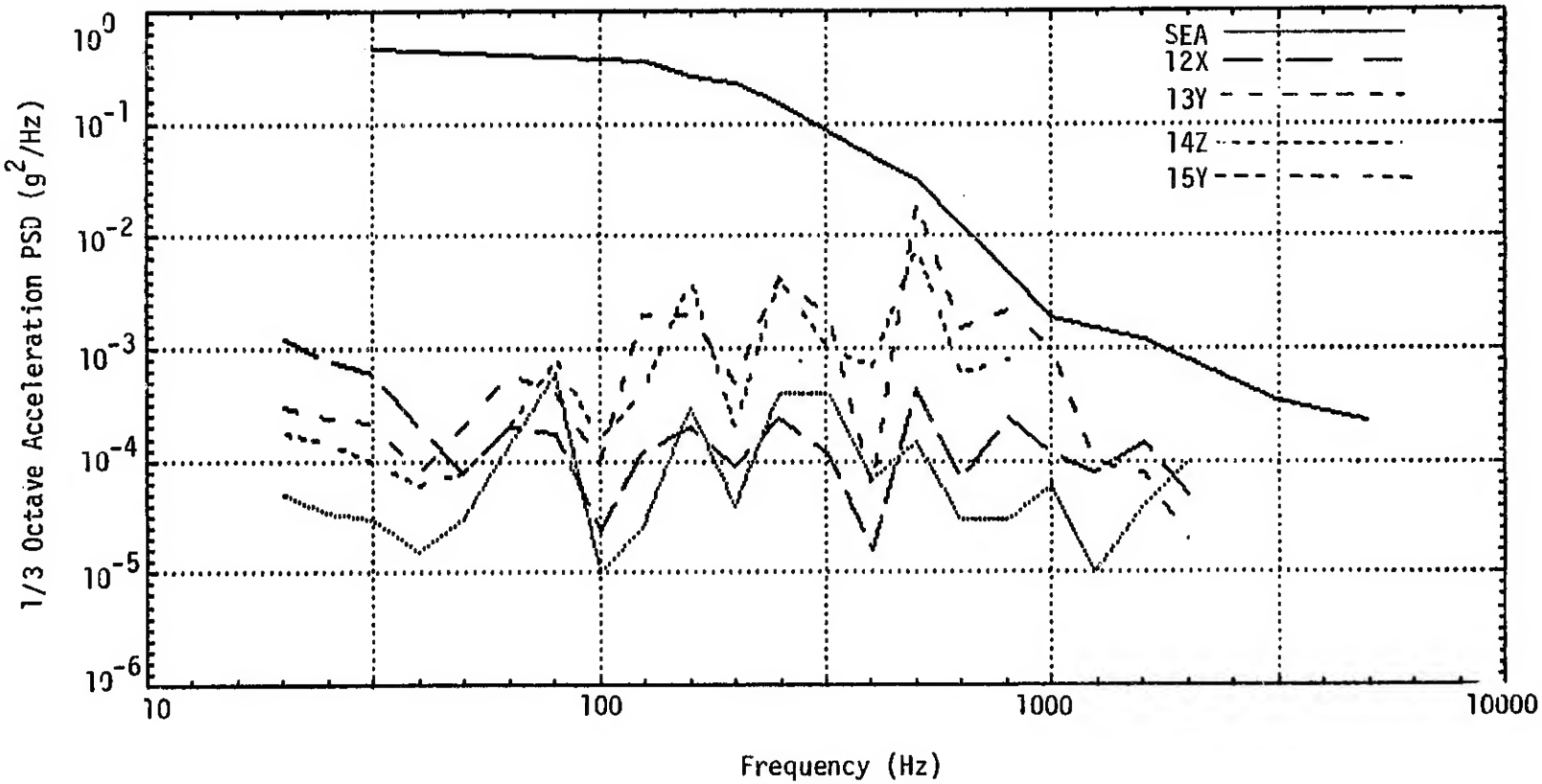

Figure 7 - Comparison of Initial SEA Prediction and Acoustic Test Measurements for Element 2

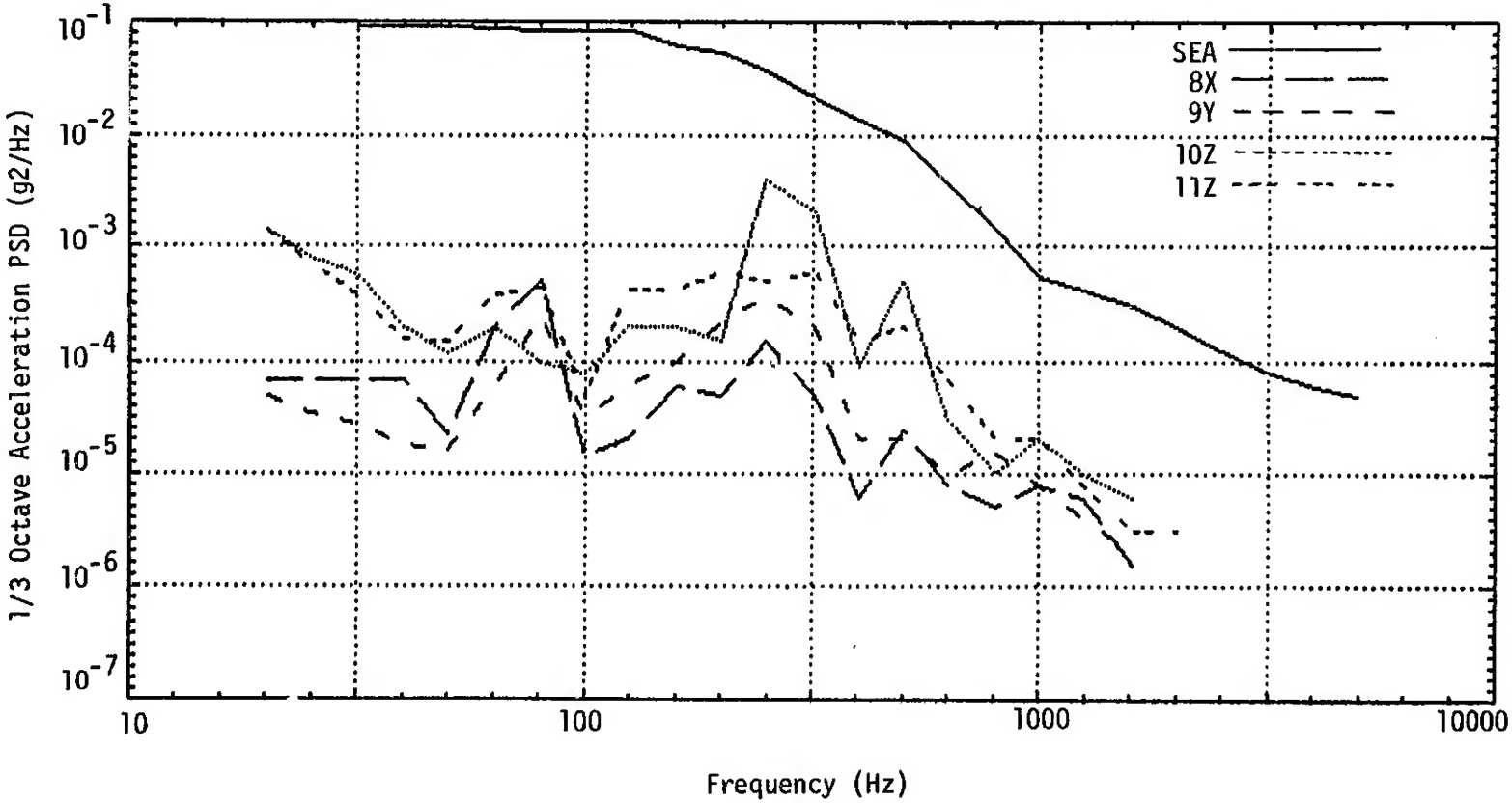

Figure 8 - Comparison of Initial SEA Prediction and Acoustic Test Measurements for Element 3

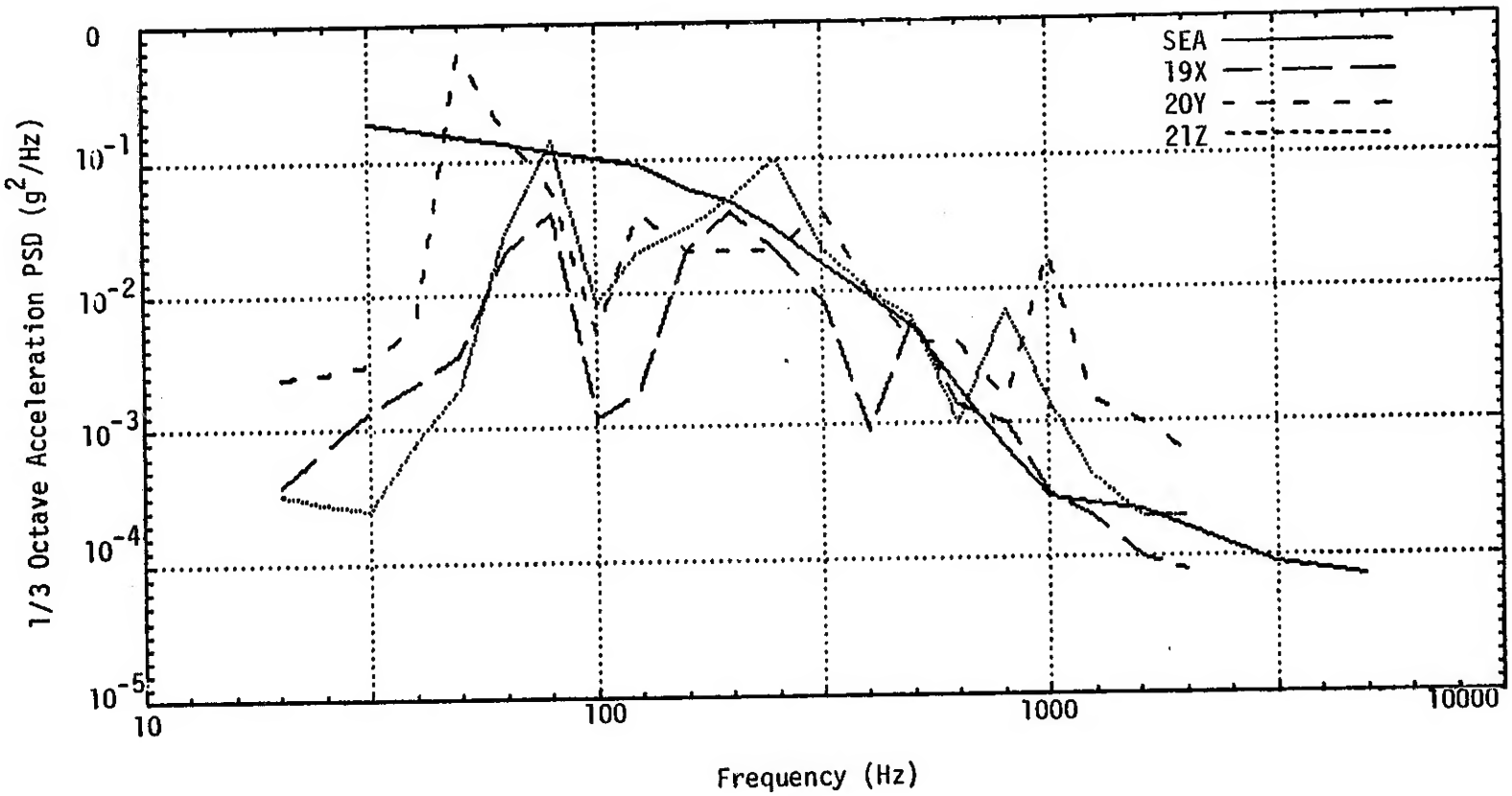

Figure 9 - Comparison of Initial SEA Prediction and Acoustic Test Measurements for Element 4

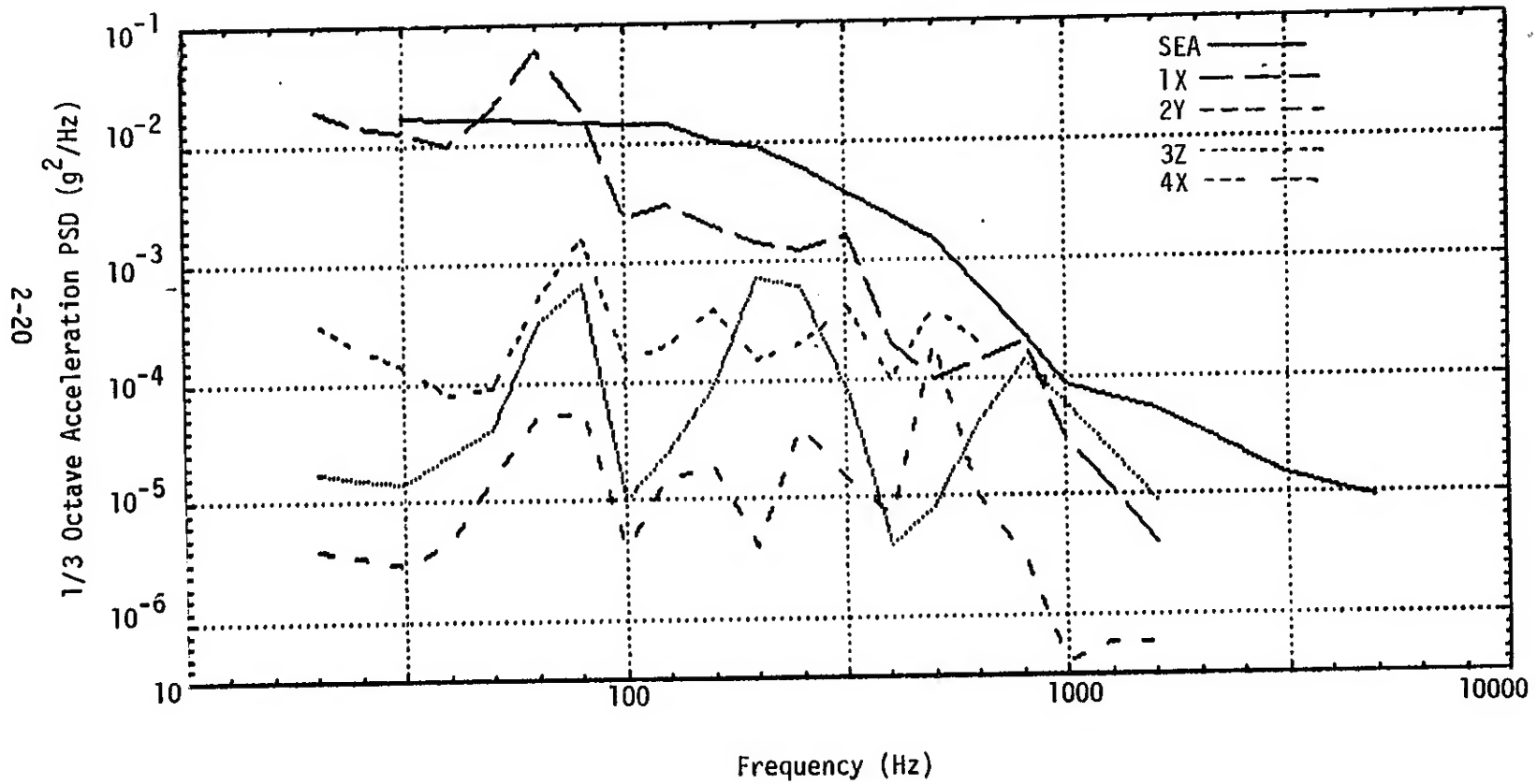

Figure 10 - Comparison of Initial SEA Prediction and Acoustic Test Measurements for Element 5

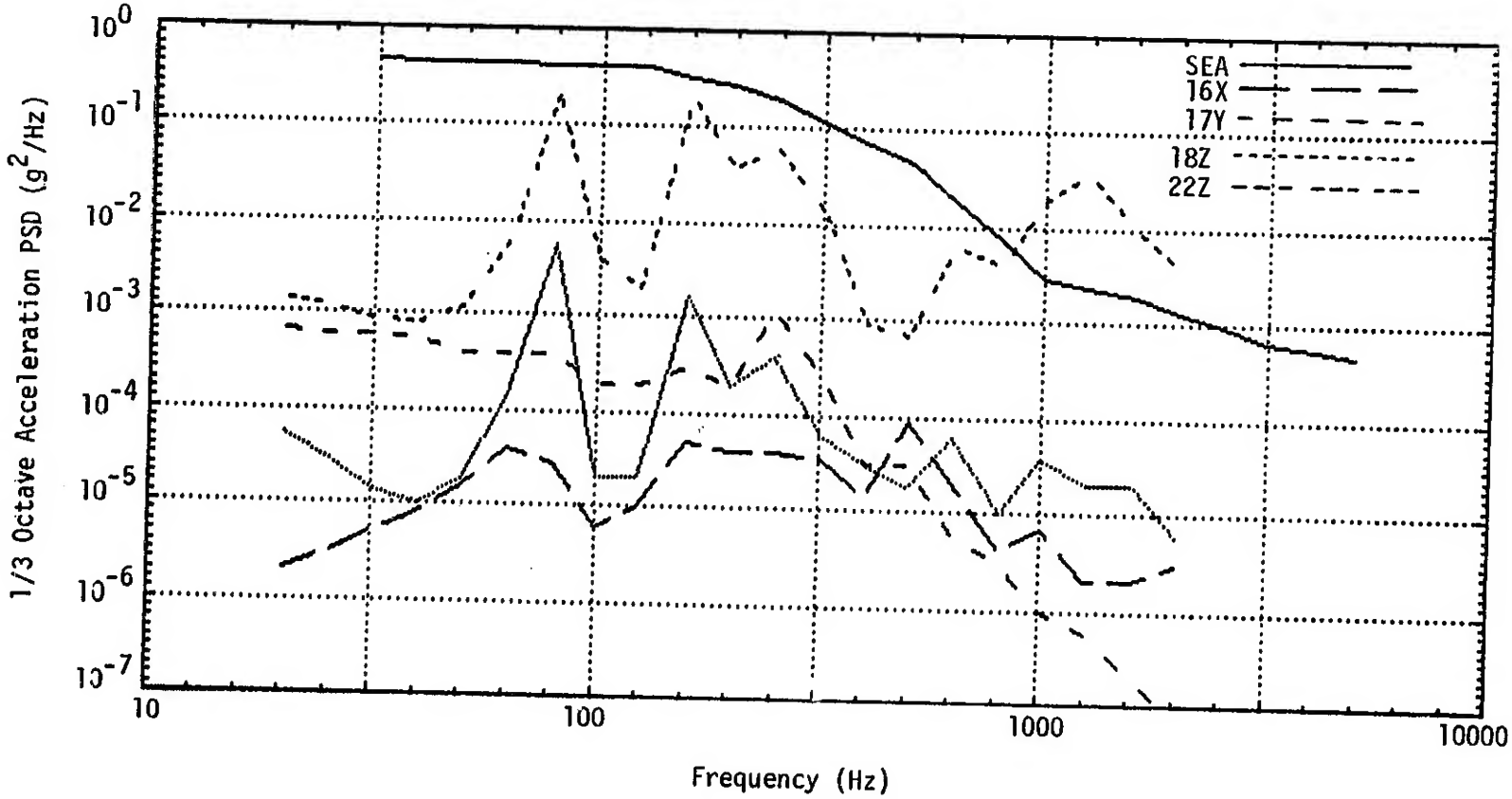

Figure 11 - Comparison of Initial SEA Predictions and Acoustic Test Measurements for Element 6

Table 2

MEA ACOUSTIC TEST
ACCELEROMETER LOCATIONS

Accelerometer No.		Axis	Location	Sketch No.
1X 2Y 3Z	Triaxial	X Y Z	Bottom Cold Plate and Battery Box Input	1
4X		X	Battery Box Response	1 & 2
5X 6Y 7Z	Triaxial	X Y Z	Primary Structure, Center Post	3
8X 9Y 10Z	Triaxial	X Y Z	Upper Cold Plate, Data Acquisition Box Input	4
11Z		Z	Upper Cold Plate, Coolant Pump Input	4
12X 13Y 14Z	Triaxial	X Y Z	Distributor Input, Vertical Panel	5
15Y		Y	Distributor	5
16X 17Y 18Z	Triaxial	X Y Z	EAC Input	1 & 6
19X 20Y 21Z	Triaxial	X Y Z	Solenoid Valve Equipment Panel	6
22Z		Z	EAC Cap Response	6
23Y		Y	Equipment Panel Accumulator Input	6
24X		X	Thermal Panel #10	7
25Y		Y	Thermal Panel #6	7

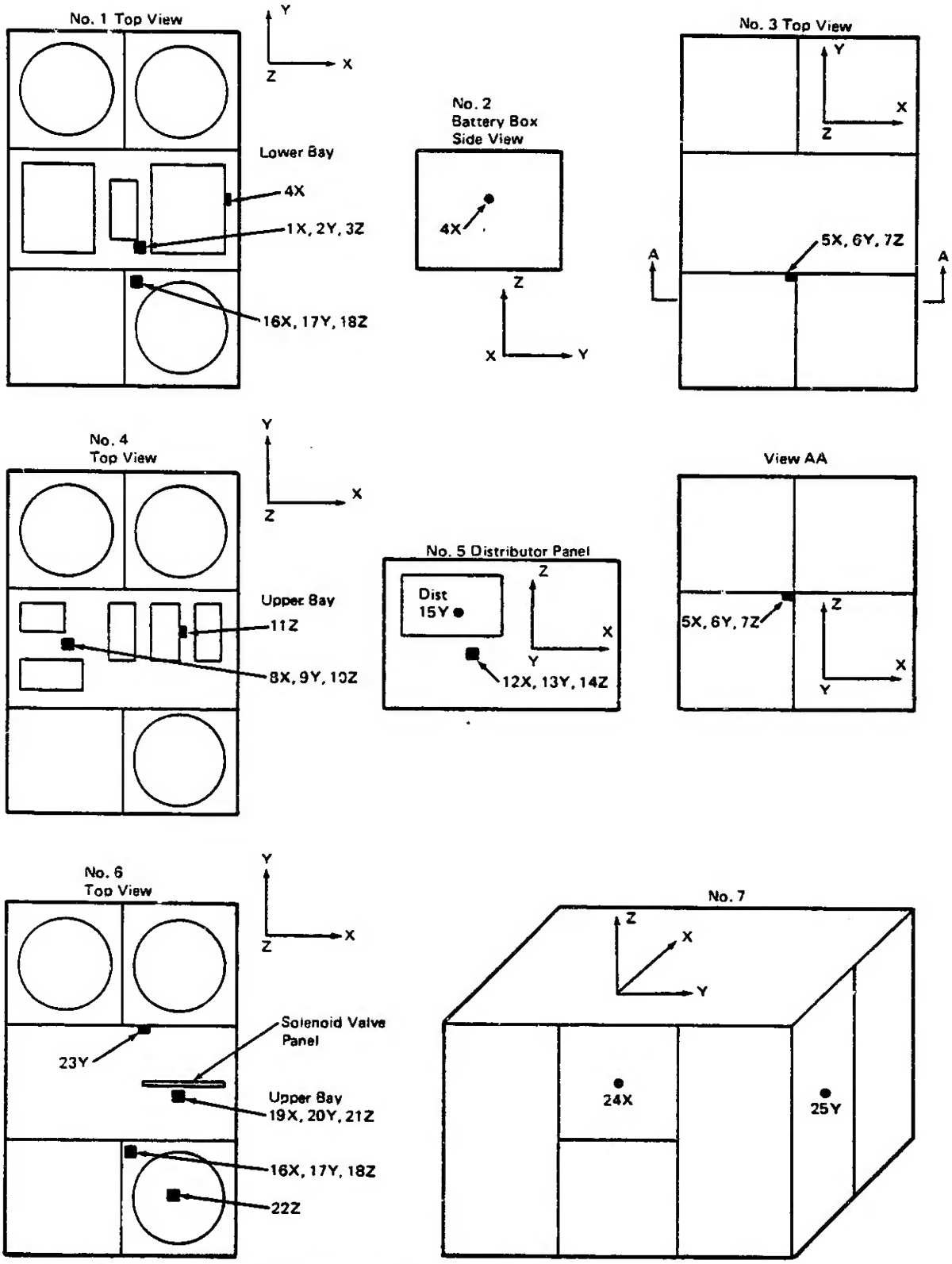

Figure 12 - MEA Accelerometer Location Sketches

representation of all plate subelements as one term. At lower frequencies the individual plates have much lower modal densities than represented by the gross element model, which is a single "smeared" plate.

For element 2, the SEA predictions are higher than the acoustic measurements, but the predicted response curve is seen to be converging to the measured value at higher frequencies (Figure 7). Measurements 12X and 14Z are parallel to the structure surface and are not appropriate for comparison with the SEA predictions. 13Y and 15Y measured accelerations perpendicular to the surface at two locations. When averaged they create a slightly higher resultant PSD. The slight difference in the prediction shape and the relative trends at higher frequencies seem to indicate that both frequency-dependent damping and coupling factor changes are required.

The SEA prediction for element 3 is also higher than the acoustic test data. The general trends of the test data and the predictions are about the same except for a slight difference at higher frequencies (Figure 8). As in element 2, frequency-dependent damping and changes in the coupling factor should resolve the disagreement.

The SEA prediction for element 4 matches up well with the acoustic test data (Figure 9). Again the prediction starts to fall below the data at higher frequencies, indicating variable damping is required. However, since element 4 is coupled through element 3, the indicated reduction in the predicted response for element 3 would cause a drop in the prediction for element 4. This seems to indicate that there is an alternate energy path not accounted for in the modeling. The alternate energy path could be due to additional acoustic excitation by the internal MEA acoustic field or through mechanical coupling to element 1 (photographs of the test article seem to indicate the latter possibility).

In element 5, the SEA prediction is much higher than measurements 2Y, 3Z, and 4X located on the battery cold plate and battery box, and only slightly higher than data point 1X (Figure 10). Measurements 1X and 2Y monitored

motions in the plane of the structure and represent cross axis responses which do not apply to the SEA predictions. The convergent trend in the higher frequencies of the prediction and data from 3Z (normal to the battery mounting plate) indicates frequency-dependent damping is required. The generally high predictions indicate the coupling assumed in the analysis was excessive.

The prediction for element 6 is much higher than the test data (Figure 11). Variable damping appears to be required because of the steeper slope of the prediction when compared to measurement 18Z (normal to the experiment plate). 16X and 17Y represent cross axis PSD's relative to the SEA prediction. Measurement 22Z appears to have a gain problem. Comparing data from 18Z and 22Z, the measured responses at lower frequencies follow the same trends except for a difference of two decades on the PSD (Figure 13). At lower frequencies the two responses should be nearly identical, because the stiffness of the canister structure dictates primarily rigid body motions between the two measurements. At higher frequencies the shell response of the canister creates an additional departure from the SEA because it is not represented as an element in the model.

The extra energy predicted by the SEA model for element 6 indicates that the coupling between elements 1 and 6 is not as large as predicted. The higher SEA prediction could also indicate that modeling of the experiment canister as part of the element was not correct. Treatment of the experiment and the experiment canister as mass loadings that reduce the modal density of the experiment panel could be more appropriate. This was the approach used in modeling elements 2, 3, 4 and 5. SEA response predictions may normally be expected to have good accuracy when there are more than 20 modes per analysis bandwidth (or above the ring frequency for a curved structure). Only element 1 meets this criterion in the 200-2000 Hz frequency range.

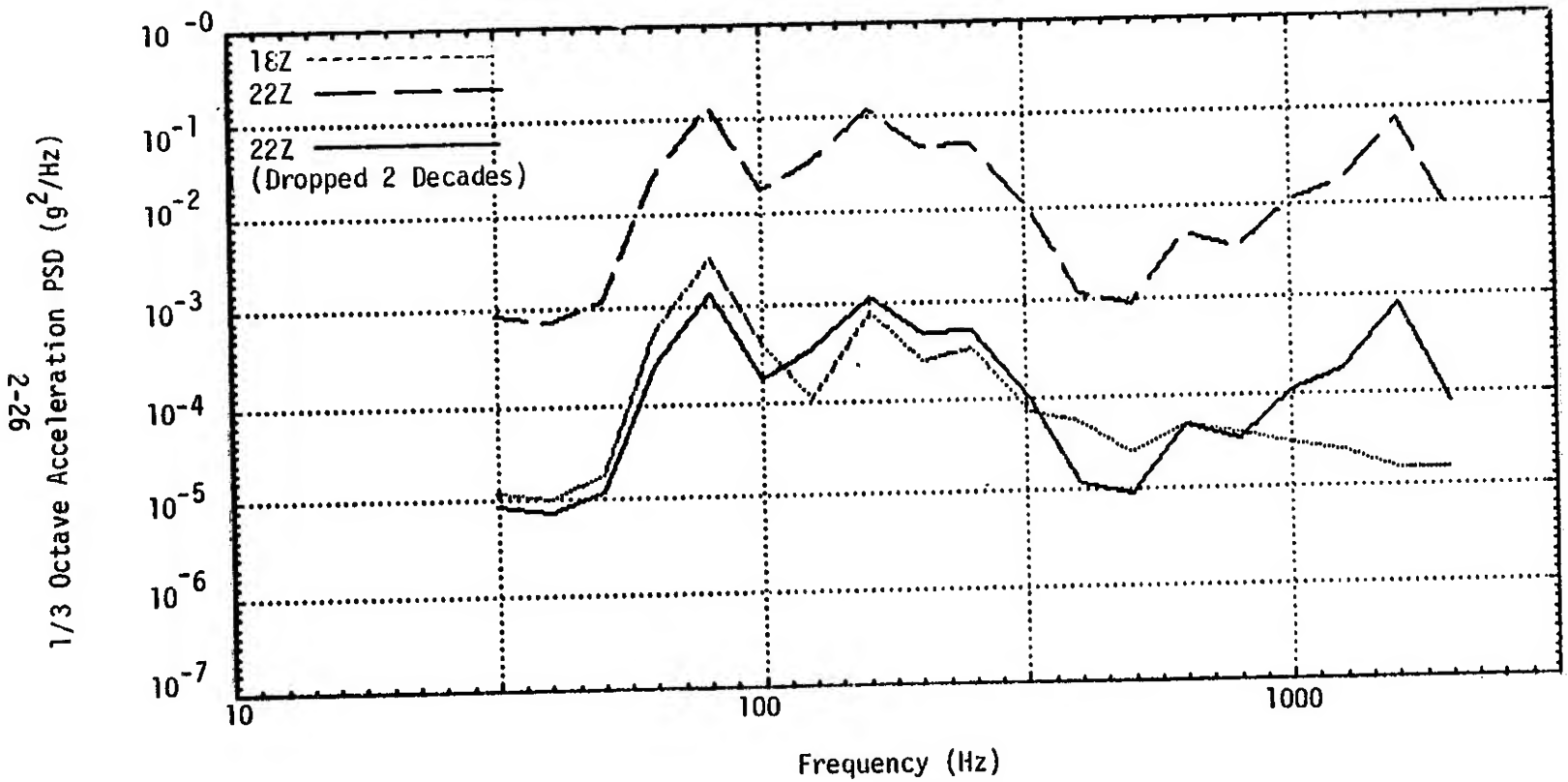

Figure 13 - Comparison of Test Measurements 18Z and 22Z

Section 3

REFINEMENTS TO SEA MODEL

The main refinements indicated by the comparison of the SEA predicted response levels with acoustic measurements were re-evaluation of the element damping and element-to-element coupling. Modifications to the modeling of the modal density of element 6 and identification of a possible alternative energy path to element 4 were also of interest.

The modal density of element 6 was recalculated by assuming the experiments and experiment housings act primarily as mass loadings that stiffen the experiment mounting plates. Stiffening of the plates results in a lowering of the modal density of element 6. An increase in stiffness by a factor of 2 and a corresponding reduction in the modal density by $1/\sqrt{2}$ was used in the calculations for elements 2-5. The recalculated modal density of element 6 is

$$n_6 = 0.080 \text{ modes/Hz}$$

In the process of reviewing the structural drawings, one joint connecting element 1 to element 4 was found. This new path is diagrammed in Figure 14. The element coupling coefficient was calculated as explained in the section on structural coupling.

$$\phi_{14} = 0.0008$$

The system of equations describing the SEA model for acoustic excitation now becomes:

$$\begin{bmatrix} \alpha_{11} & \alpha_{12} & \alpha_{13} & \alpha_{14} & \alpha_{15} & \alpha_{16} \\ \alpha_{21} & \alpha_{22} & & & & \\ \alpha_{31} & & \alpha_{33} & \alpha_{34} & & \\ \alpha_{41} & & \alpha_{43} & \alpha_{44} & & \\ \alpha_{51} & & & & \alpha_{55} & \\ \alpha_{61} & & & & & \alpha_{66} \end{bmatrix} \begin{Bmatrix} E_1 \\ E_2 \\ E_3 \\ E_4 \\ E_5 \\ E_6 \end{Bmatrix} = \begin{Bmatrix} S_1 \\ 0 \\ 0 \\ 0 \\ 0 \\ 0 \end{Bmatrix}$$

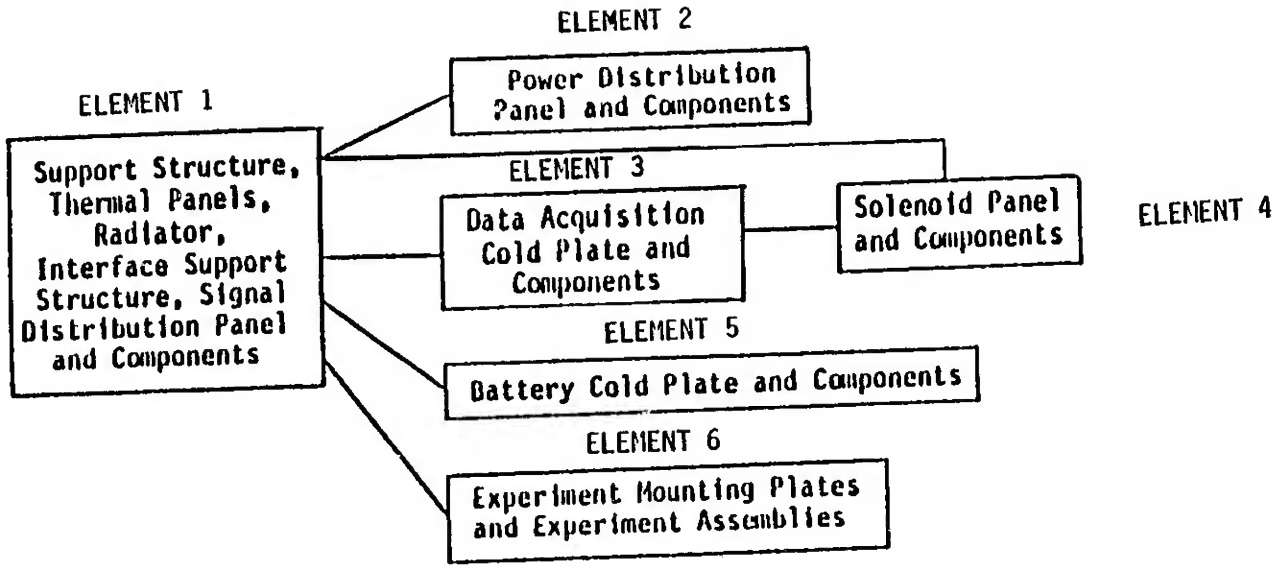

Figure 14 - SEA Model Elements for Acoustic Test Configuration

The need for frequency-dependent damping in elements 2-6 was indicated by the difference in slope of the predicted response levels and the test measurements at higher frequencies. It was decided to decrease the rate of damping as a function of frequency above 250 Hz. The starting frequency of the decrement and the rate of decreasing damping were based on measurements from an acoustic test of Saturn IVB/V interstage panels (Ref. 3). The equation used to calculate the decreasing damping was of the form:

$$\eta = 4.7687 * f^{-1.11640}$$

where:

f = frequency (Hz)

η = element loss factor

A graph of the damping values used in elements 2-6 is shown in Fig. 15.

The basis for revising the element coupling coefficients was the observation that the outer element (element 1) prediction agreed with the test data, but the internal elements' response levels were overpredicted. The element coupling coefficients used in the analysis assumed the bolted connections between elements would be comparable to rigid joints. It is apparent this assumption was not valid. Methods of calculating the energy transfer through bolted connections were not found in any of the literature on SEA. It was therefore decided to arbitrarily reduce the coupling coefficient calculated for a rigid connection by an order of magnitude (10) for the bolted connections. The energy path between the main resonator of element 1 (the thermal panels) and elements 2, 3, 5 and 6 passes through an intermediate subelement (the internal support structure-ISS). The thermal panels and elements 2, 3, 5 and 6 are connected to the ISS by bolted connections. The "double" bolted joints in the energy transmission path seem to result in a reduction of the rigid joint coupling coeffieient by a factor of 100.

The reduced coupling coefficients due to the "double" bolted joints are as follows:

Figure 15. Damping Parameter for SEA Elements 2-7

$$\phi_{12} = 0.0048/\sqrt{f}$$
$$\phi_{13} = 0.0116/\sqrt{f}$$
$$\phi_{14} = 0.0008/\sqrt{f}$$
$$\phi_{15} = 0.0093/\sqrt{f}$$
$$\phi_{16} = 0.020/\sqrt{f}$$
$$\phi_{34} = 38.6/\sqrt{f}$$

The SEA predictions were recalculated using the frequency-varying damping and the reduced element coupling coefficients.

3.1 COMPARISON OF REFINED SEA RESPONSE PREDICTIONS WITH MEASURED ACOUSTIC DATA

The revised prediction response levels are compared with all applicable test measurements in Figures 16-21.

The correlation between the predicted response levels and the test measurements remained very good for element 1 (Figure 16). The change in the system equations due to the revised damping and coupling was not enough to affect the prediction of levels in element 1 with any significance.

For element 2, the SEA prediction now shows good correlation with the applicable test measurements (13Y and 15Y), except at lower frequencies (Figure 17).

The revised SEA predictions for element 3 envelopes the measured data well and shows reasonably good correlation with measurements 10Z and 11Z (Figure 18). The predicted response levels for element 4 with the addition of the coupling between elements 1 and 4 is shown in Figure 19. Since element 4 is also coupled to element 3, the reduction in the calculated response of element 3 also lowered the response of element 4. The agreement between the measured data and the predicted response in the initial response calculations appears to be coincidental. The present predicted response levels are uniformly lower than the test data; however, the general trends of the SEA prediction and the test measurements match up very well for frequencies above 100 Hz.

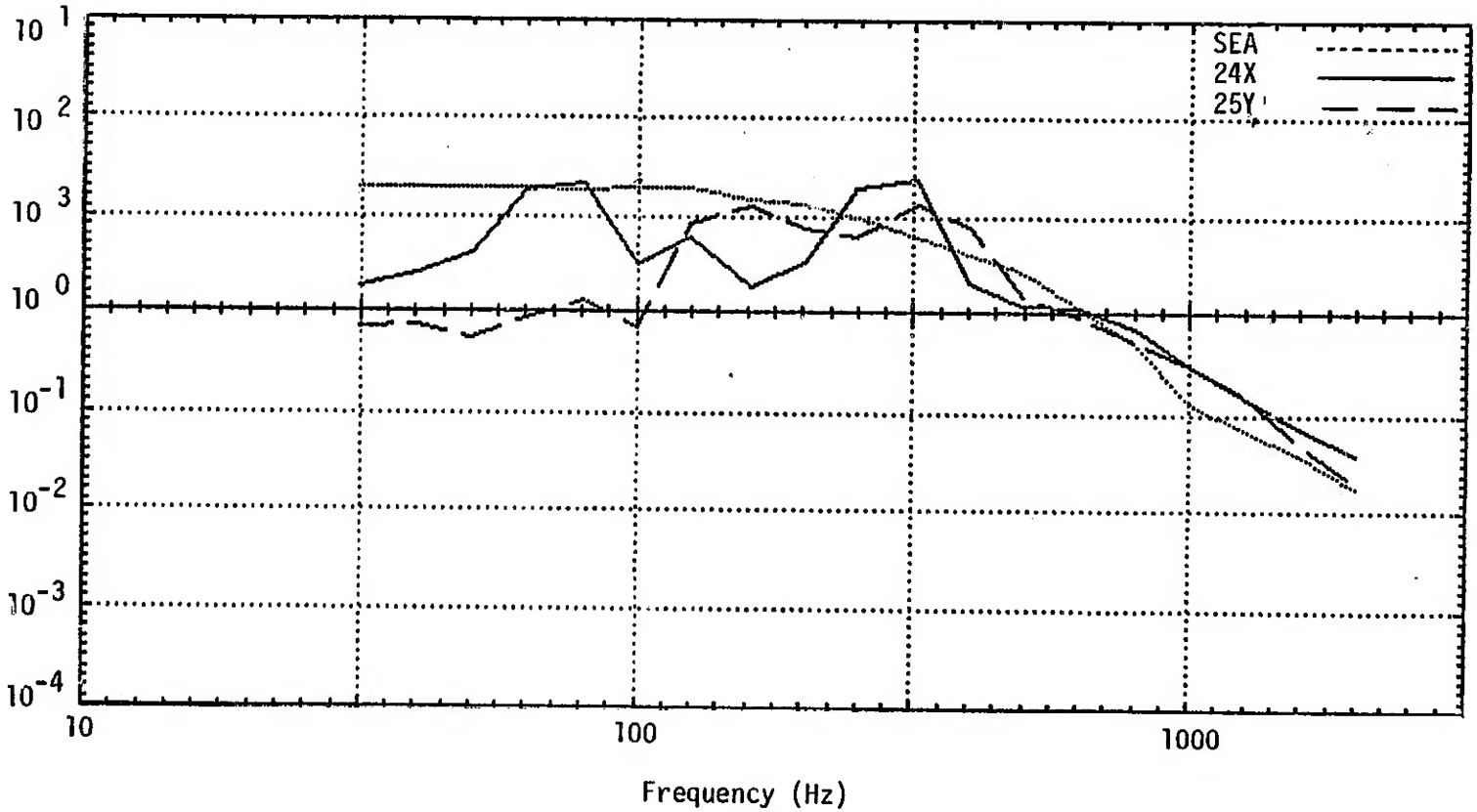

Figure 16 - Comparison of Revised SEA Model Prediction and All Applicable Test Data for Element 1

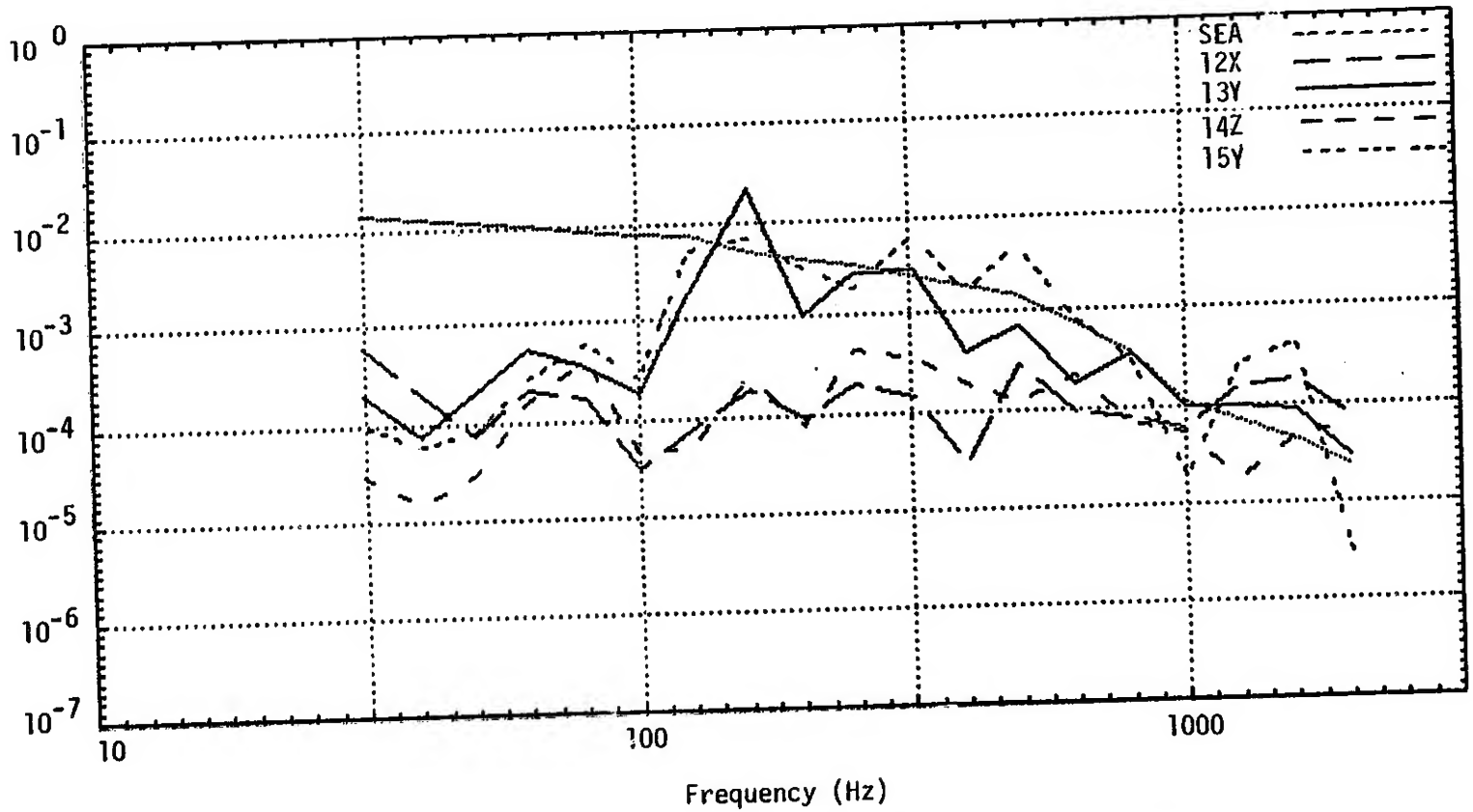

Figure 17 - Comparison Revised SEA Model Prediction and All Applicable Test Data for Element 2

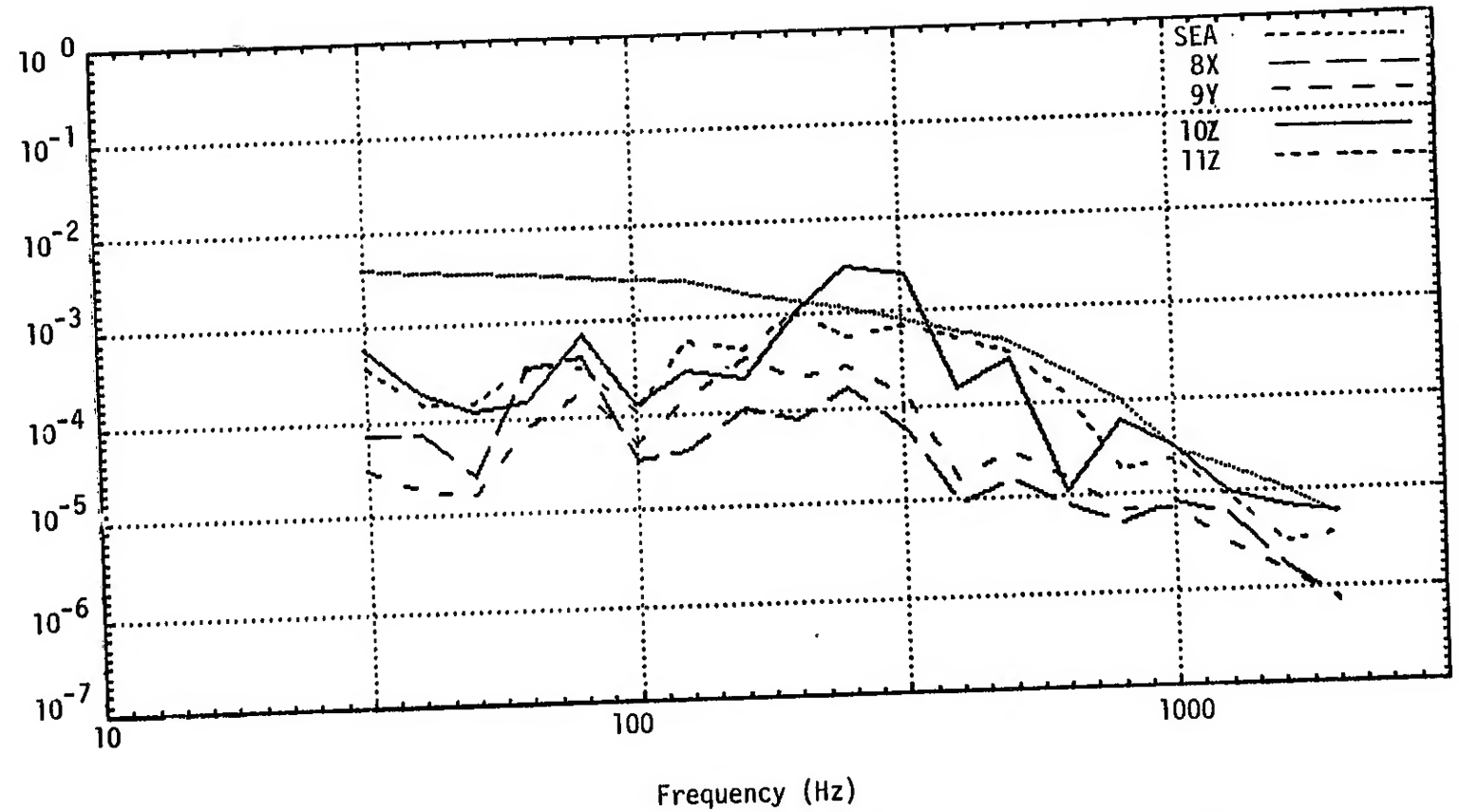

Figure 18 - Comparison of Revised SEA Model Prediction and All Applicable Test Data for Element 3

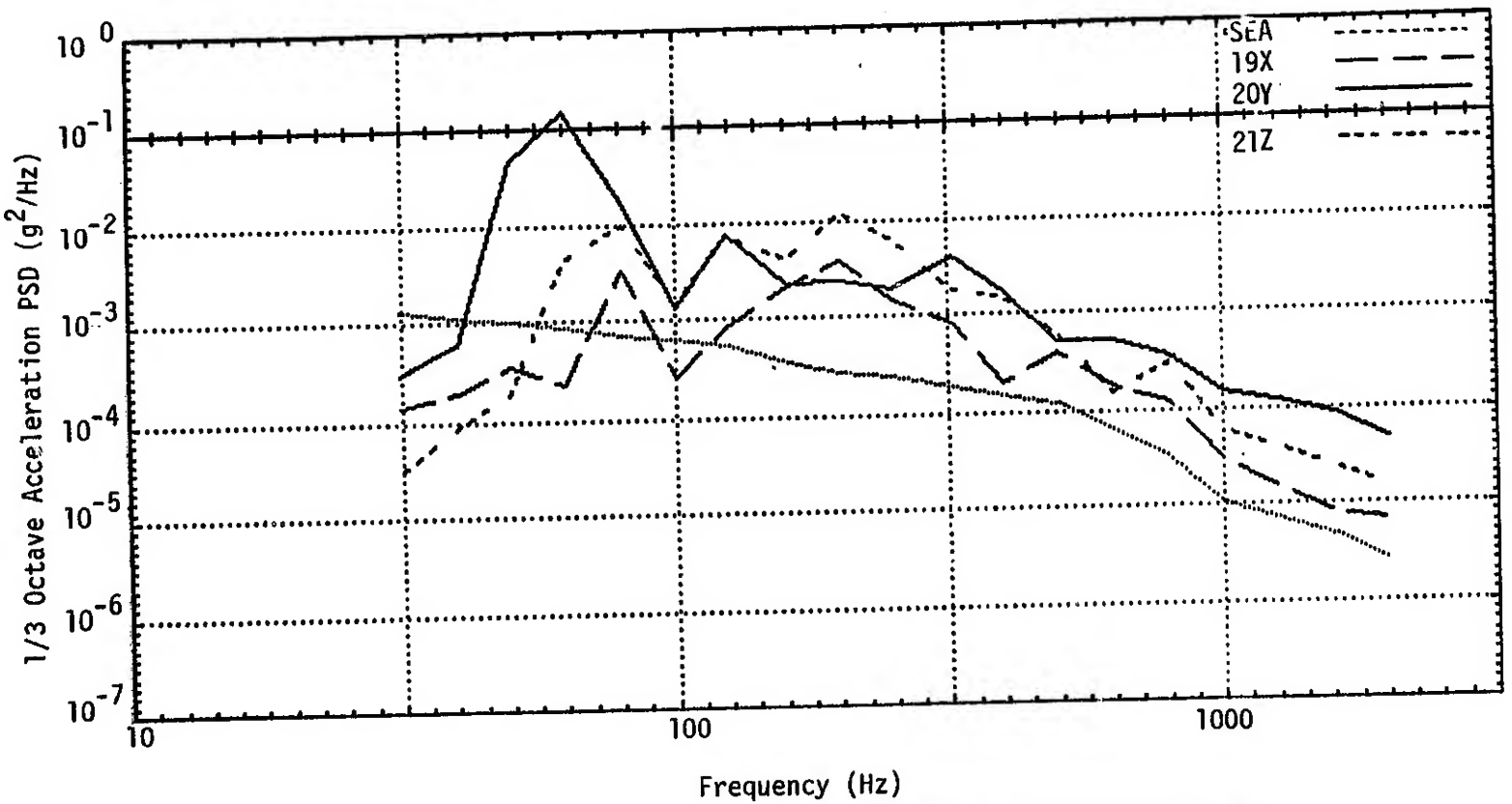

Figure 19 - Comparison of Revised SEA Model Prediction and All Applicable Test Data for Element 4

This seems to indicate that the use of frequency-dependent damping was correct, but that there is still an energy path not accounted for in the modeling. This energy path could be a mechanical path through the various hard lines connected to element 4 or through an acoustic path between element 1 and Element 4.

In element 5, the SEA prediction matches 3Z fairly well (Figure 20). The peaks and notches indicated in measurement 3Z could be due to subelements that are modeled as mass loads in the SEA model. The largest test measurement (1X) is parallel to the surface of the battery plate and is not applicable to SEA predictions.

The SEA response prediction for element 6 is still much higher than the test data (Figure 21). The use of variable damping adjusted the slope of the prediction so that the shape now matches that of the test measurements. The reduced coupling and reduced modal density has lowered the prediction levels, but more energy is still being represented in the model than is indicated by the test measurement. This could be explained by the location of the accelerometers in a corner of the experiment mounting plate. A more appropriate data comparison point would be one located in the center of the experiment mounting plate, which would be expected to register higher response levels. The data from measurement 22Z was dropped from consideration because of the suspected gain problem.

In summary, the use of frequency-dependent damping seems to have been justified. The trends of all the predictions match the test data at frequencies above 100 Hz. The reduction in coupling also seems to be justified because the predicted response levels match the test measurements except as noted in the above comparisons.

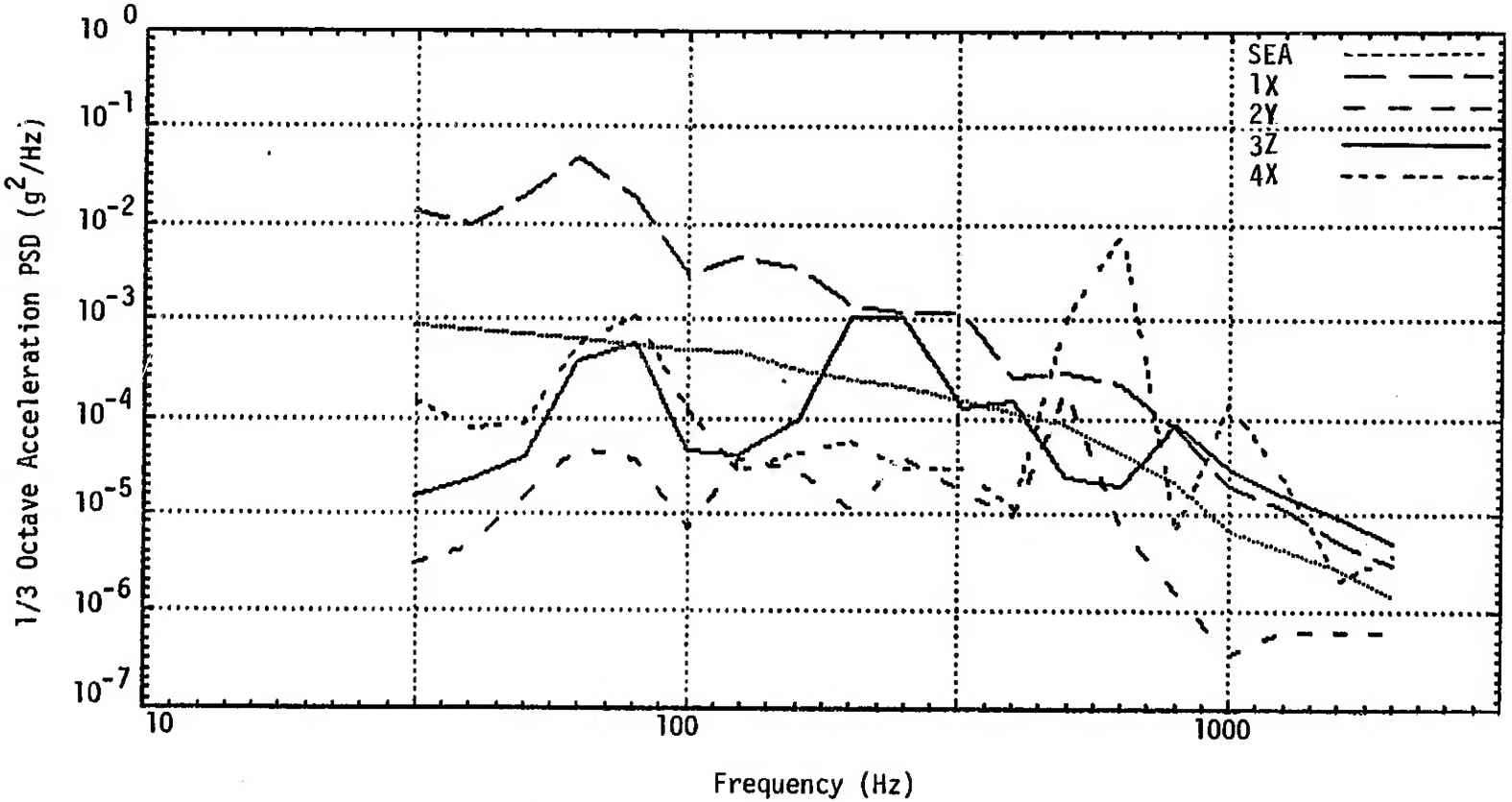

Figure 20 - Comparison of Revised SEA Model Prediction and All Applicable Test Data for Element 5

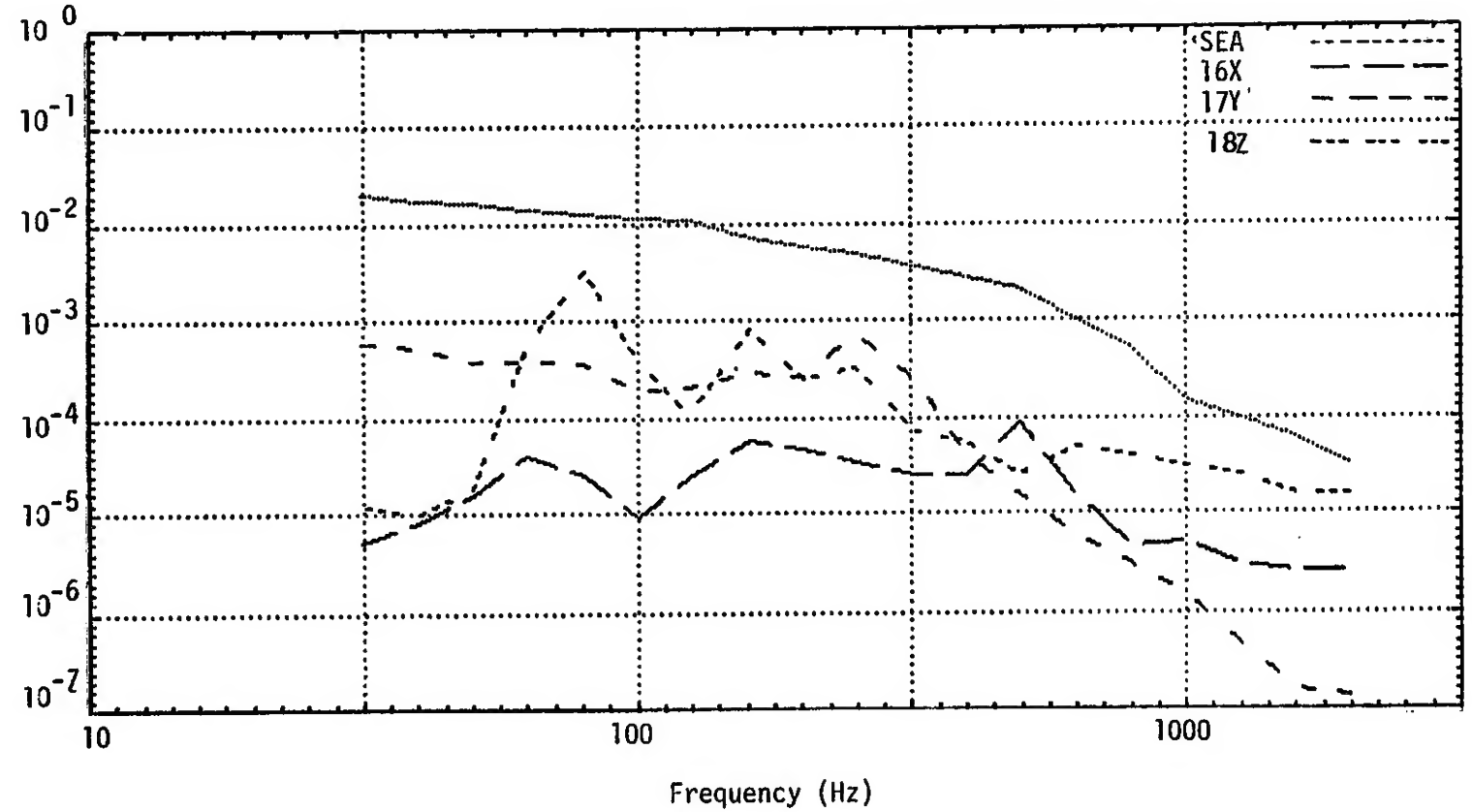

Figure 21 - Comparison of Revised SEA Model Prediction and All Applicable Test Data for Element 6

Section 4

VIBRATION PREDICTIONS FOR PAYLOAD/SUPPORT STRUCTURE WITH COMBINED ACOUSTIC/MECHANICAL EXCITATION

The main structure to be modeled is the MEA package modeled in Phase I of this contract (Vibration Predictions for a Payload/Support Structure with Acoustic Excitation). The Mission Peculiar Equipment (MPE) Support Structure has been attached to the MEA package for the SEA model for Phase II. Since the system of equations describing the model is linear, the predicted responses of the SEA model elements to mechanical excitation alone can be computed and added to the predicted responses for acoustic input alone to obtain a prediction for the combined acoustic and mechanical input response levels.

The response of the MPE Support Structure to flight conditions was provided by MSFC. This known response was used as mechanical input to the system by the support structure.

4.1 MODELING

As in Phase I, the MEA package was divided into six elements. The MPE support structure was lumped into a seventh element. The structural element breakdown, element identification numbering, and connectivity are shown in Figure 22.

For the seven-element system, the SEA response equations become:

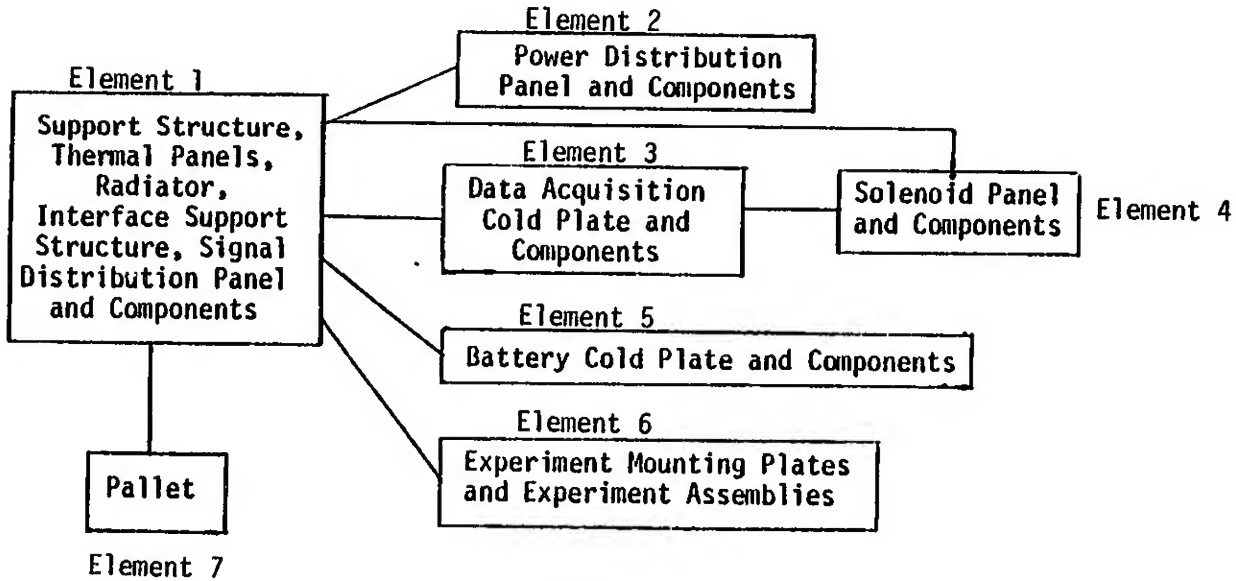

Figure 22. SEA Model Elements for Flight Configuration

$$\begin{vmatrix} \alpha_{11} & \alpha_{12} & \alpha_{13} & \alpha_{14} & \alpha_{15} & \alpha_{16} & \alpha_{17} \\ \alpha_{21} & \alpha_{22} & & & & & \\ \alpha_{31} & & \alpha_{33} & \alpha_{34} & & & \\ \alpha_{41} & & \alpha_{43} & \alpha_{44} & & & \\ \alpha_{51} & & & & \alpha_{55} & & \\ \alpha_{61} & & & & & \alpha_{66} & \\ \alpha_{71} & & & & & & \alpha_{77} \end{vmatrix} \begin{Bmatrix} E_1 \\ E_2 \\ E_3 \\ E_4 \\ E_5 \\ E_6 \\ E_7 \end{Bmatrix} = \begin{Bmatrix} S_1 \\ S_2 \\ S_3 \\ S_4 \\ S_5 \\ S_6 \\ S_7 \end{Bmatrix}$$

There is no external acoustic or mechanical excitation,

$$S_1 = S_2 = S_3 = S_4 = S_5 = S_6 = S_7 = 0$$

The response of element 7 is known, therefore the system of equations can be reduced.

Where $E_1 = -E_7 \frac{\alpha_{77}}{\alpha_{71}}$

then

$$\begin{vmatrix} \alpha_{12} & \alpha_{13} & \alpha_{14} & \alpha_{15} & \alpha_{16} \\ \alpha_{22} & & & & \\ & \alpha_{33} & \alpha_{34} & & \\ & \alpha_{43} & \alpha_{44} & & \\ & & & \alpha_{55} & \\ & & & & \alpha_{66} \end{vmatrix} \begin{Bmatrix} E_2 \\ E_3 \\ E_4 \\ E_5 \\ E_6 \end{Bmatrix} = \begin{Bmatrix} -E_1\alpha_{11} - E_7\alpha_{17} \\ -E_1\alpha_{21} \\ -E_1\alpha_{31} \\ -E_1\alpha_{41} \\ -E_1\alpha_{51} \\ -E_1\alpha_{61} \end{Bmatrix}$$

or

$$\begin{vmatrix} \alpha_{12} & \alpha_{13} & \alpha_{14} & \alpha_{15} & \alpha_{16} \\ \alpha_{22} & & & & \\ & \alpha_{33} & \alpha_{34} & & \\ & \alpha_{43} & \alpha_{44} & & \\ & & & \alpha_{55} & \\ & & & & \alpha_{66} \end{vmatrix} \begin{Bmatrix} E_2 \\ E_3 \\ E_4 \\ E_5 \\ E_6 \end{Bmatrix} = E_7 \begin{Bmatrix} \alpha_{11}\left(\frac{\alpha_{77}}{\alpha_{71}}\right) - \alpha_{17} \\ \alpha_{21}\left(\frac{\alpha_{77}}{\alpha_{71}}\right) \\ \alpha_{31}\left(\frac{\alpha_{77}}{\alpha_{71}}\right) \\ \alpha_{41}\left(\frac{\alpha_{77}}{\alpha_{71}}\right) \\ \alpha_{51}\left(\frac{\alpha_{77}}{\alpha_{71}}\right) \\ \alpha_{61}\left(\frac{\alpha_{77}}{\alpha_{71}}\right) \end{Bmatrix}$$

This system of equations can then be solved for

$$E_2 = E_7 \left(\frac{\alpha_{21}}{\alpha_{22}}\right)\left(\frac{\alpha_{77}}{\alpha_{71}}\right)$$

$$E_5 = E_7 \left(\frac{\alpha_{51}}{\alpha_{55}}\right)\left(\frac{\alpha_{77}}{\alpha_{71}}\right)$$

$$E_6 = E_7 \left(\frac{\alpha_{61}}{\alpha_{66}}\right)\left(\frac{\alpha_{77}}{\alpha_{71}}\right)$$

$$E_4 = E_7 \frac{\left(\frac{\alpha_{77}}{\alpha_{71}}\right)\left[\alpha_{41} - \alpha_{43}\left(\frac{\alpha_{31}}{\alpha_{33}}\right)\right]}{\alpha_{44} - \alpha_{43}\left(\frac{\alpha_{34}}{\alpha_{33}}\right)}$$

$$E_3 = E_7 \left(\frac{\alpha_{31}}{\alpha_{33}}\right)\left(\frac{\alpha_{77}}{\alpha_{71}}\right) - E_4\left(\frac{\alpha_{34}}{\alpha_{33}}\right)$$

4.2 DAMPING

A loss factor of $\eta = 0.01$ was assigned to element 1. For elements 2-7, η was uniform below 250 Hz and frequency dependent above 250 Hz. The loss factor used in the prediction was calculated using the following:

$$\eta_{2\text{-}7} = 0.01 \qquad f < 250 \text{ Hz}$$

$$= 4.7687 * f^{-1.11640} \qquad 250 \text{ Hz} < f$$

4.3 MODAL DENSITY

The modal density of elements 1 through 6 are the same as that used in the refined SEA model for acoustic excitation.

$n_1 = 6.84$ modes/Hz
$n_2 = 0.0110$ mode/Hz
$n_3 = 0.0076$ mode/Hz
$n_4 = 0.0237$ mode/Hz
$n_5 = 0.0083$ mode/Hz
$n_6 = 0.080$ mode/Hz

Element 7 basically consists of multiple plate sections. Therefore, the element density was found using the approximate equation for the high frequency modal density of plates.

$$n_7 = \frac{1}{2\sqrt{\frac{Eg}{12\bar{w}(1-\nu^2)}}} \sum \frac{A}{t}$$

$$= 2.683 \text{ modes/Hz}$$

4.4 STRUCTURAL COUPLING

The element coupling coefficients calculated in refining the SEA model for acoustic excitation alone were used to describe coupling between elements 1 through 6. For the coupling between element 1 and element 7, reduction by an order of 10 because of the bolted joint was not used. The spacing of the bolts was not small enough to assume a connection approaching that of a rigid joint. Rather, a joint length of 3 inches was assumed around each bolt to be used in calculating the coupling coefficient. The element coupling coefficients used for the mechanical input model are as follows:

$$\phi_{12} = 0.0048/\sqrt{f}$$

$$\phi_{13} = 0.0116/\sqrt{f}$$

$$\phi_{14} = 0.0008/\sqrt{f}$$

$$\phi_{15} = 0.0093/\sqrt{f}$$

$$\phi_{16} = 0.020\ /\sqrt{f}$$

$$\phi_{17} = 0.0044/\sqrt{f}$$

$$\phi_{34} = 38.6\ /\sqrt{f}$$

where $\phi_{ij} = \phi_{ji}$

4.5 ELEMENT ENERGY

The element energy was handled as in Phase I.

Where $E_j = m_j \frac{\overline{\langle a_j^2 \rangle}}{\omega^2}$

$m_1 = 1.5936$ lb-s^2/in.

$m_2 = 0.0725$ lb-s^2/in.

$m_3 = 0.2820$ lb-s^2/in.

$m_4 = 0.0688$ lb-s^2/in.

$m_5 = 1.7358$ lb-s^2/in.

$m_6 = 1.4696$ lb-s^2/in.

$m_7 = 2.2021$ lb-s^2/in.

4.6 RESPONSE SOLUTION

The mechanical excitation input was provided by MSFC as X-axis, Y-axis, and Z-axis PDS levels (Table 3, Figure 23). The sum of the PSD levels was used as input in the SEA predictions. This was chosen since it is a more conservative approach than using the root of the sum of the squares.

Table 3

MECHANICAL INPUT TO SEA MODEL

Acceleration PSD (g^2/Hz)

FREQ	X-AXIS ($X10^{-3}$)	Y-AXIS ($X10^{-3}$)	Z-AXIS ($X10^{-3}$)	X + Y + Z ($X10^{-3}$)	$(X^2 + Y^2 + 2^2)^{1/2}$ ($X10^{-3}$)
31.5	0.11	0.9	0.15	1.16	.92
40	0.18	1.45	0.24	1.87	1.48
50	0.28	2.25	0.38	2.91	2.30
63	0.43	3.6	0.60	4.63	3.67
80	0.70	5.8	0.95	7.45	5.92
100	1.10	9.0	1.5	11.6	9.19
125	1.10	9.0	1.5	11.6	9.19
160	1.10	9.0	1.5	11.6	9.19
200	1.10	9.0	1.5	11.6	9.19
250	1.10	9.0	1.5	11.6	9.19
315	0.70	9.0	0.95	10.65	9.08
400	0.43	9.0	0.60	10.03	9.03
500	0.28	5.8	0.38	6.46	5.82
630	0.18	3.6	0.24	4.02	3.61
800	0.11	2.25	0.15	2.51	2.26
1000	0.07	1.45	0.10	1.62	1.46
1250	0.045	0.95	0.065	1.06	0.95
1600	0.029	0.60	0.040	0.67	0.60
2000	0.018	0.36	0.025	0.40	0.36

Figure 23 - Mechanical Input to the SEA Model

The response predictions for the elements were determined in each 1/3 octave bandwidth from 31.5 to 2000 Hz by solving the reduced set of equations for $\langle \overline{a_i^2} \rangle$. The acceleration spectral density levels were then found where

$$PSD(f)_i = \frac{\langle \overline{a_i^2} \rangle}{g^2 \Delta f}$$

4.7 COMPARISON OF ACOUSTIC, MECHANICAL, AND ACOUSTIC/MECHANICAL EXCITATION RESPONSES

The predicted MEA element PSD response levels for acoustic excitation, mechanical excitation, and combined mechanical/acoustic input are shown in Figures 24-30. They show the mechanical input has no effect on the SEA predicted response levels at lower frequencies, but becomes increasingly significant as the frequency gets higher.

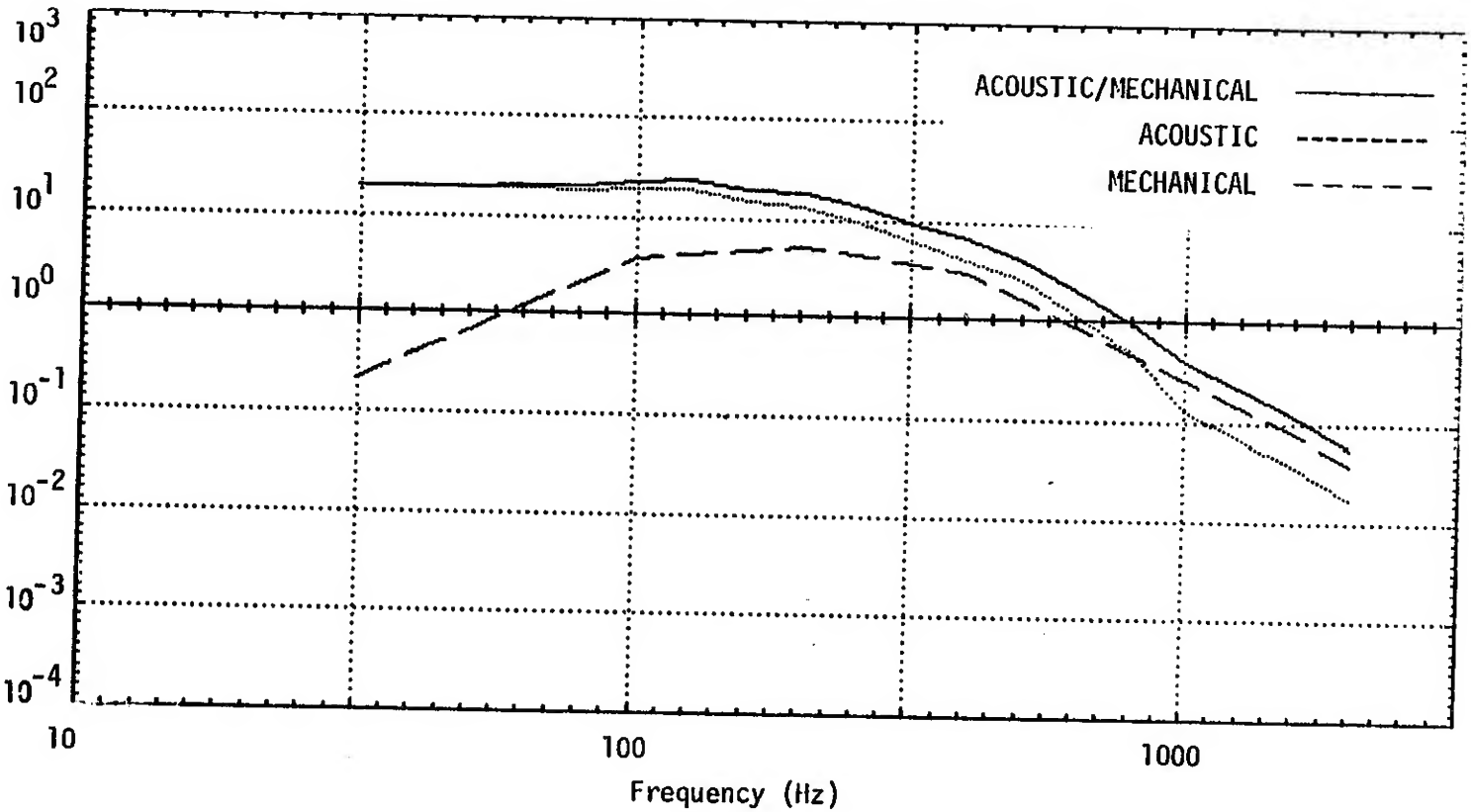

Figure 24 - SEA Response Predictions for Element 1 With Acoustic, Mechanical, and Acoustic/Mechanical Input

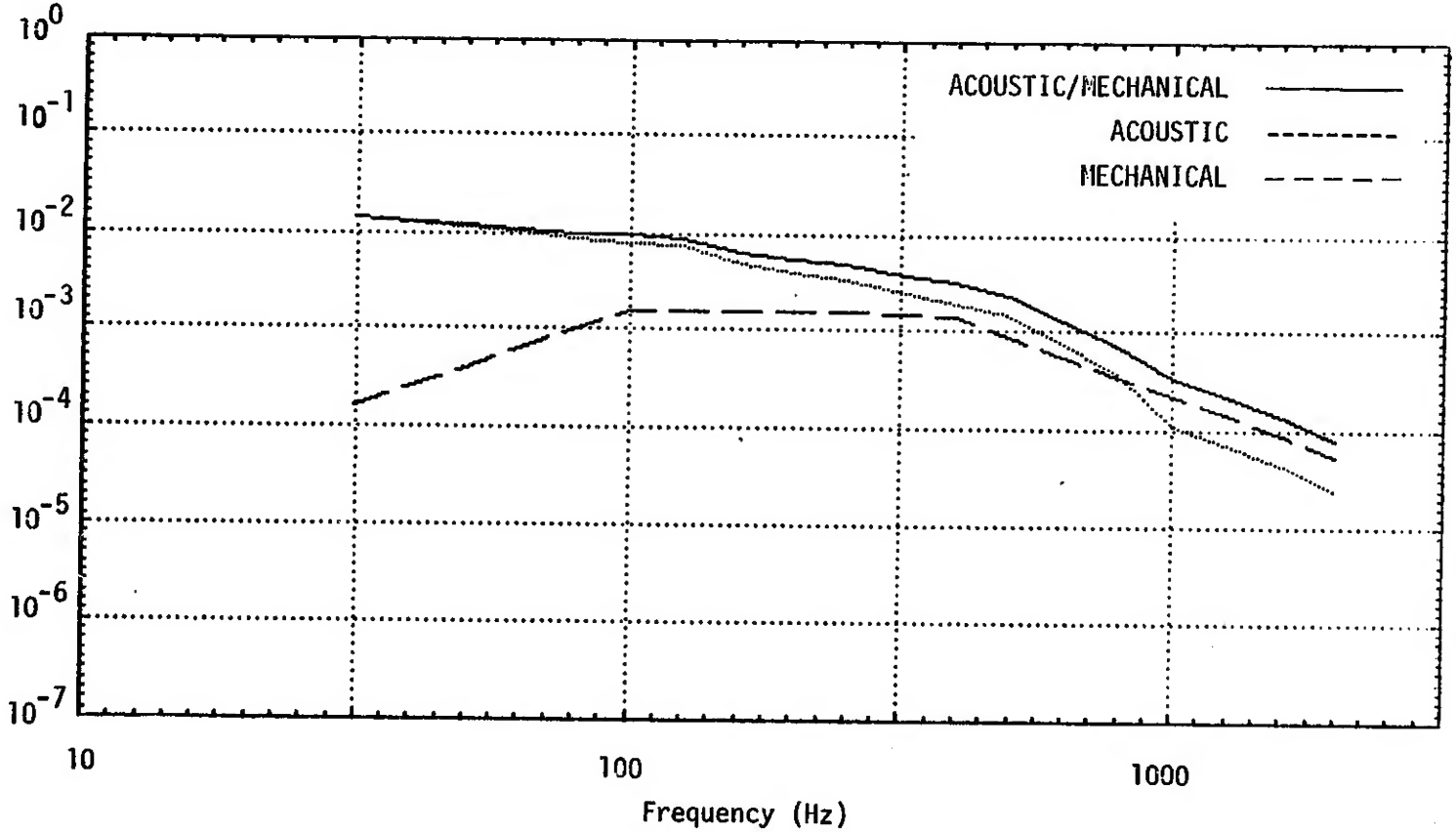

Figure 25 - SEA Response Predictions For Element 2 With Acoustic, Mechanical, and Acoustic/Mechanical Input

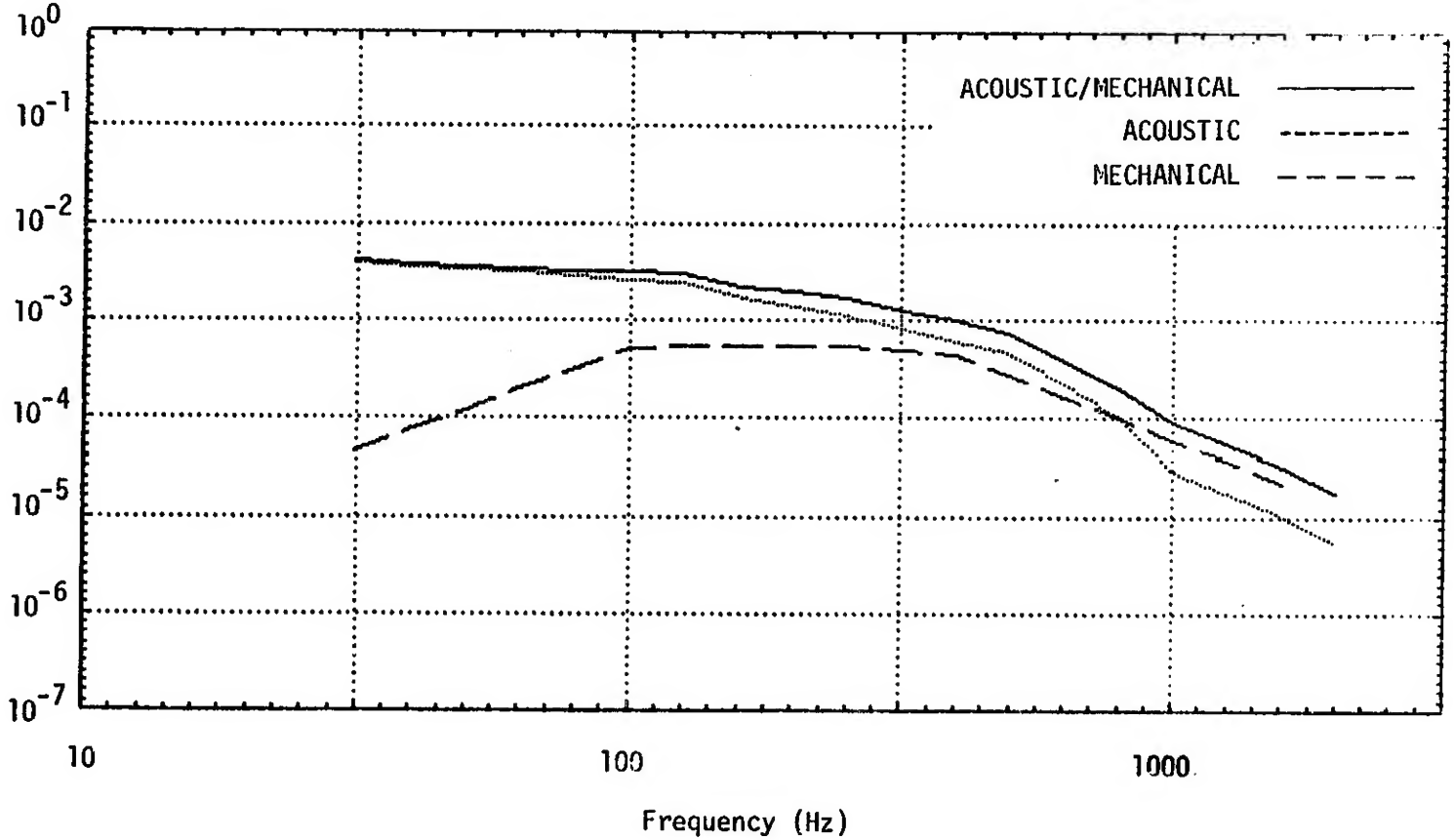

Figure 26 - SEA Response Predictions For Element 3 With Acoustic, Mechanical, and Acoustic/Mechanical Input

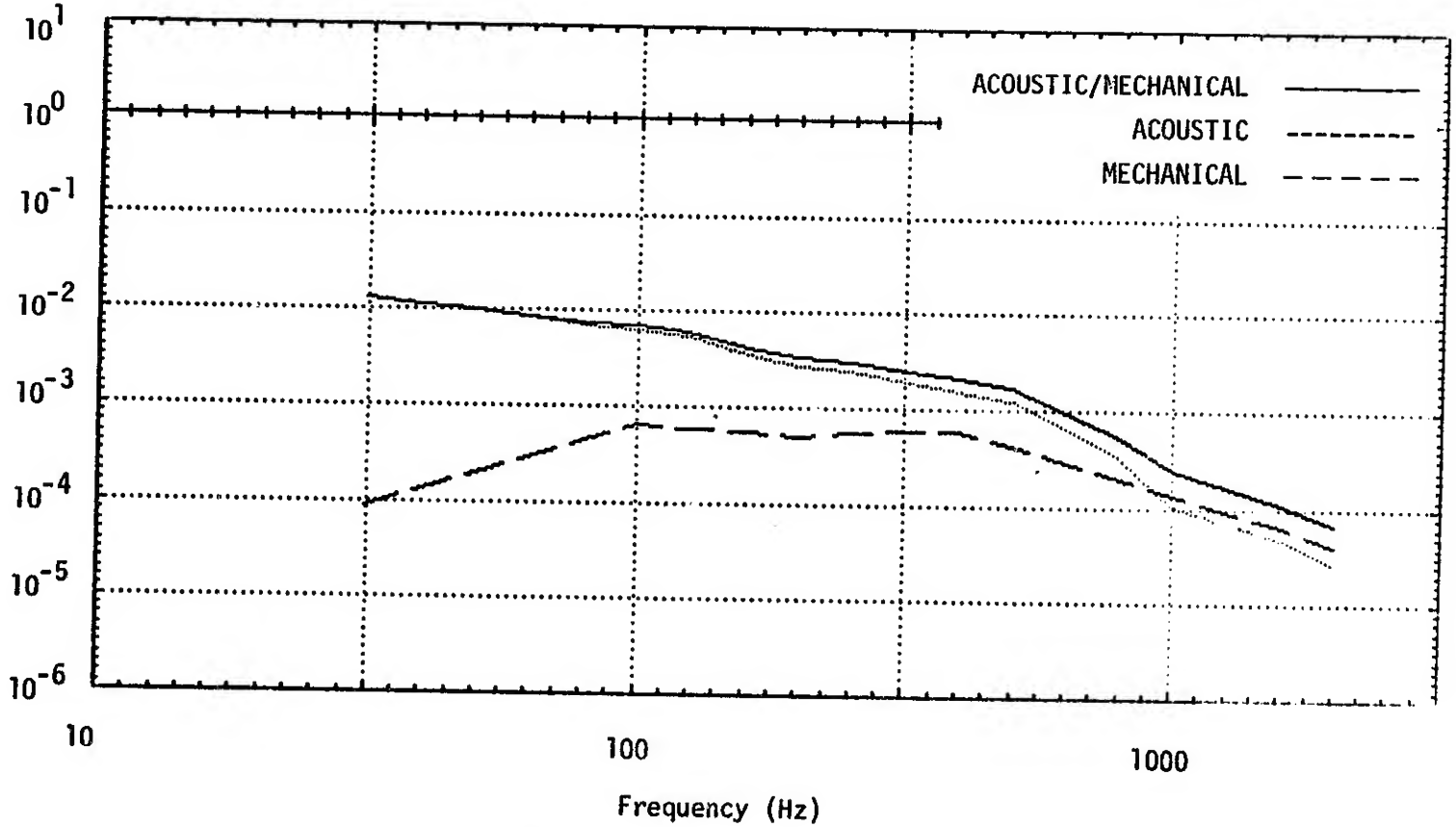

Figure 27 - SEA Response Predictions For Element 4 With Acoustic, Mechanical, and Acoustic/Mechanical Input

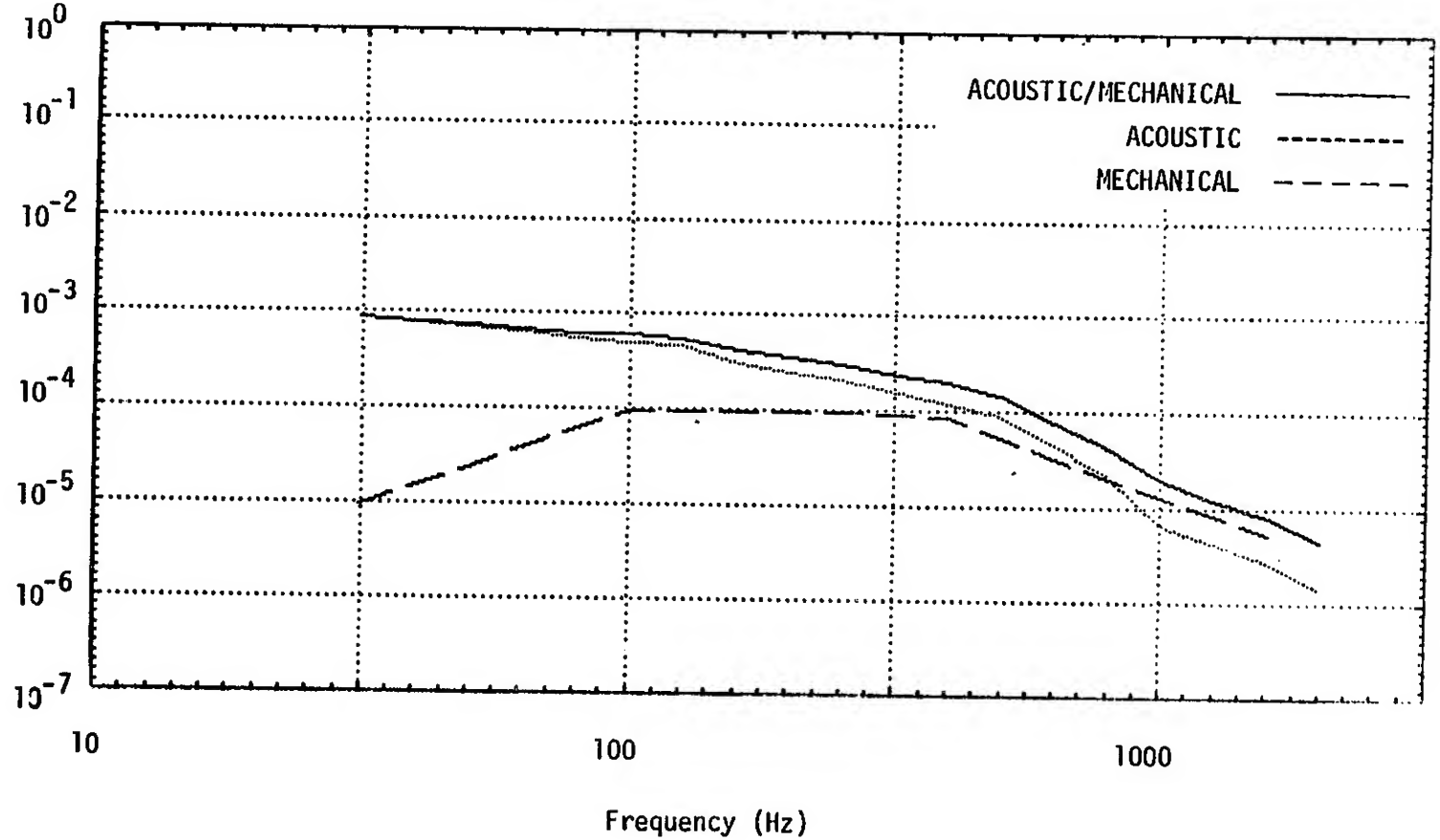

Figure 28 - SEA Response Predictions For Element 5 With Acoustic, Mechanical, and Acoustic/Mechanical Input

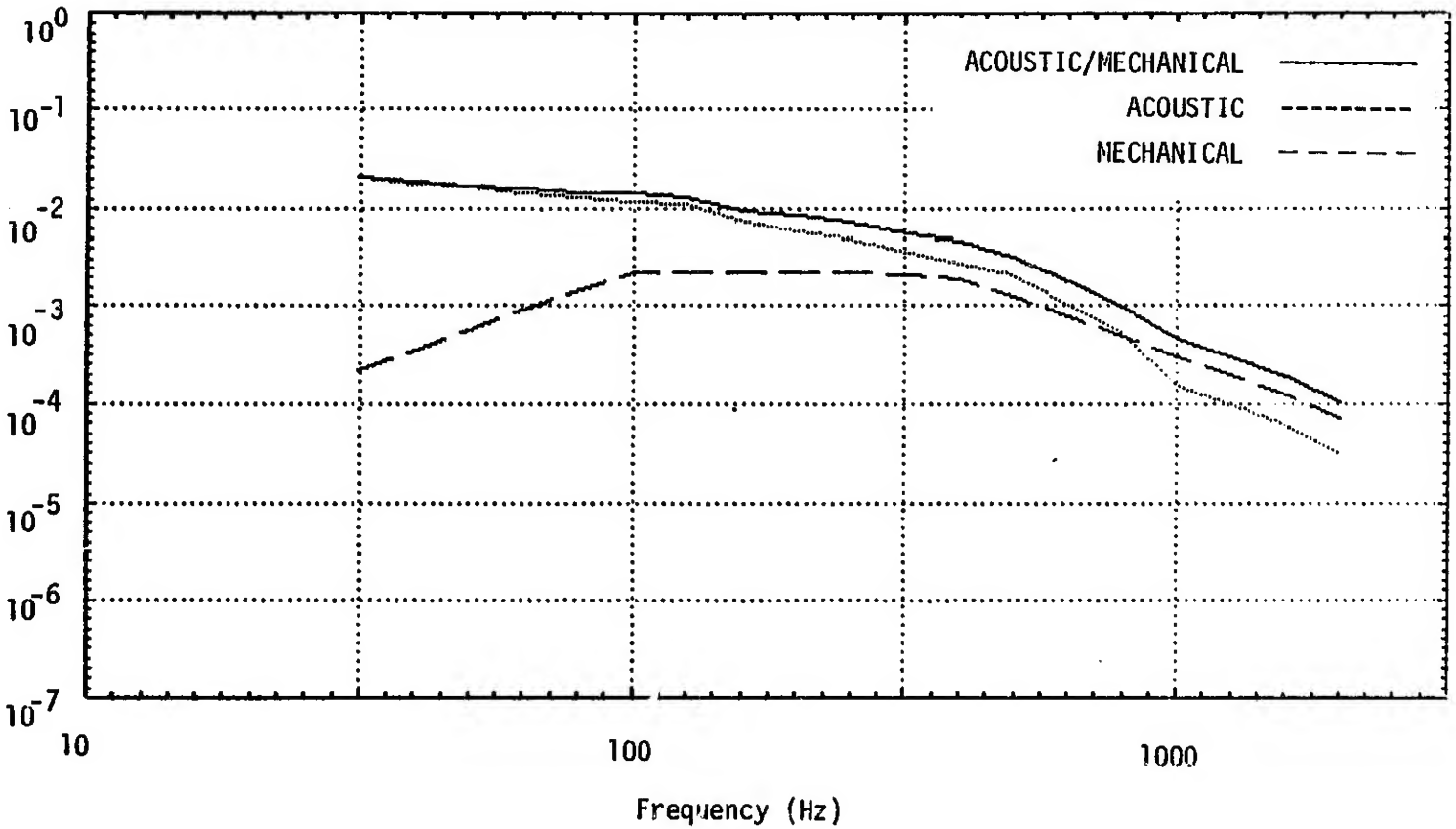

Figure 29 - SEA Response Predictions For Element 6 With Acoustic, Mechanical, and Acoustic/Mechanical Input

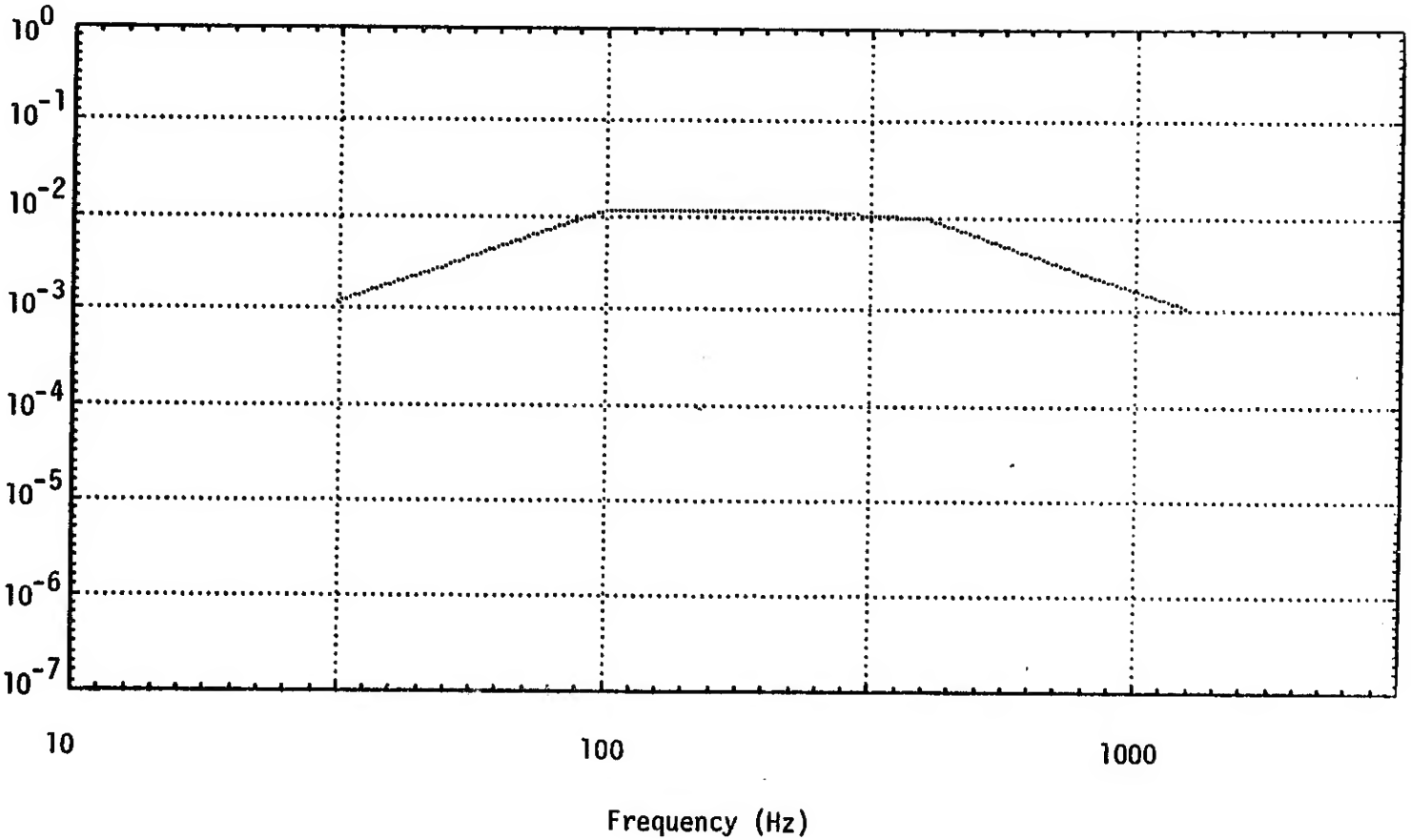

Figure 30 - Acceleration PSD Level For Element 7 Used As Mechanical Input For SEA Model

Section 5

CONCLUSIONS

In the course of this phase of the study, conclusions were reached about the materials experiment assembly which was analyzed and about the application of SEA to payload vibration predictions. The following statements may be made, with regard to this prediction effort, which reflect observations on both points.

1) The SEA predicted the response of primary structure to acoustic excitation quite well over a fairly wide frequency range when compared with the experiment.

2) The SEA overpredicted the response of most internal structures when coupling factors were based on the existing body of SEA data.

3) The SEA predicts that the contribution of mechanically induced random vibration to the total MEA response will not be significant except at higher frequencies.

4) In most cases, two factors appear to be responsible for the overprediction:
   a) Modal coupling factors at the joints were substantially lower than in the literature.
   b) Damping was frequency dependent.

5) The power flow paths to the solenoid panel were not sufficiently definable to permit adequate resolution of the prediction errors.

From these statements the general conclusion is that the SEA method has produced a prediction adequate for component specification purposes in all

but one case. Further work is needed to enlarge the body of data on internal losses, joint losses, and on modal coupling factors for various joint types, if accuracy is to be improved. In spite of this difficulty, SEA has the potential for replacing specific extrapolation methods for high frequency random vibration environmental predictions.

Section 6
APPLICATIONS GUIDELINES

1) Define response information required.

2) Partition system into elements compatible with responses of interest.

3) Identify energy sources and energy paths between elements.

4) Calculate

   i) Element damping values.

   ii) Element modal densities.

   iii) Element-to-element structural coupling coefficient.

   iv) Define acoustic and mechanical energy sources.

5) Solve SEA system of equations for element energies.

6.1 MODELING

In applying SEA techniques, care should be taken in dividing the system structures into suitable elements. The number of elements and the sub-structure boundaries represented by the elements should be selected to best provide the desired response information. When choosing the model elements, two main limitations on the SEA technique should be considered.

First, there is a tradeoff between the size of the structure represented by the element and the accuracy of the SEA prediction. This tradeoff is a result of the general proportional relationship between structure size and mode count. If there are many modes of an element excited in a frequency band, the energy of the system can be assumed to be distributed throughout the element and the modes within the analysis band. Averaging over the element

when this occurs then gives a valid approximation of actual response behavior. Therefore the larger the substructure being modeled, the higher the mode count, and consequently the SEA element's average representation of the behavior of the substructure is improved.

In order to obtain the high number of modes in each element, model elements are chosen as relatively gross portions of the structure. The finer details are "smeared" over the substructure in the SEA element model. Parts of the structure where response predictions are not required are lumped into other pieces of the structure for modeling. The averaging quality of SEA makes the lumping of structural parts possible since averaging over multiple parts of the structure is as valid as averaging over one part of the structure. As an added advantage, the lumping of substructures into one SEA element model results in a reduction of the bookkeeping required.

The second limitation to be considered in modeling is the comparability of SEA predicted responses to the information required at discrete points on the structure. Since SEA averages over the entire element, the SEA calculated response is more comparable to the behavior of some points of the structure, while the prediction is unrepresentative of the behavior of other points of the structure. For example, if a plate element is of interest, the response of the center of the plate would be roughly comparable to the result of an SEA analysis while the response at a corner of the plate would not be comparable. The use of SEA and the interpretation of the analysis results should be weighted by the two aforementioned considerations.

The partitioning of the structure to determine SEA element boundaries and boundary conditions is made along actual structural joints or discontinuities. These divisions are made in accordance with the principles of SEA stated in the introduction.

Once the structure has been partitioned, all energy sources should be identified. The energy input to each element is usually identifiable as acoustic

or mechanical input. The definition of energy sources is used not only to indicate all sources of excitation of the system, but is also useful as an aid in limiting the size of the model. Any part of the structure that has a net energy flow of zero can be used as a model boundary.

For example, consider the case where one element of the model is the external skin of an airframe. It is not necessary to include the entire external skin in the SEA model. The amount of external skin area to include in the model can be defined so there is a zero net flow of energy across the boundaries of this element of the model. Selection of the correct skin area yields a balanced system, with the energy flowing into the model subsystem mechanically from the remainder of the structure equal to the energy transported mechanically out of the subsystem. In many cases this ideal condition can be approximately achieved by establishing the model boundaries at points halfway between major structural loading points, i.e., halfway between attach points of two adjacent equipment panels, halfway between the panel attach point and a fuel tank bulkhead, halfway between the panel attach point and a large component, etc. The effect on response predictions of incorrect estimation of the skin area will be in essentially direct proportion to the error: selection of an area too large by 10% will result in predicted levels (g^2/Hz) that are too high by approximately 10%.

6.2 DAMPING

A damping or internal loss factor for each element is required in the analysis. Although much work has been done in investigating damping, the choice of loss factor for each element is still fairly arbitrary. This arbitrariness is due to the loss factor representing not only the damping of the element but also the joint dissipations not included in the coupling loss factor and losses due to radiation. The best means of deriving the representation of the internal losses in the elements is engineering judgement based on experience gained from testing similar structures.

6.3 MODAL DENSITY

The number of modes per frequency of an element is known as the element

modal density. This parameter is used to calculate the number of modes present in each SEA analysis band. Equations for calculating the approximate modal density of various structure shapes are available (Table 4, Ref. 4). Using these equations, the approximate modal density of each SEA element can be found. Since the structure represented by each SEA element is generally large, the element may actually be composed of hundreds of individual parts. The modeling of all these parts by one SEA element is made possible by the averaging assumptions of SEA. A simple algorithm is used to calculate the SEA modal density parameter. The gross structure is decomposed into its various individual parts. These parts in turn can be decomposed, if necessary, into simpler components (i.e. an open box can be decomposed into five plate components). The modal density of these simple substructures can be calculated using the approximate modal density equations. The modal density of the SEA element is then represented by summation of the modal densities of the various parts.

One alternative to using the approximate equations is the packaged computer programs available that calculate the closed form solution of the mode count of various common structures (i.e. liquid-filled cylinders, pinned-end cylinders). A second alternative is the use of the results of low-frequency modal analysis tests. This can only be used where a low-frequency modal analysis of the structural element has been previously conducted. The results of the modal analysis are used to plot modes vs. mode number. If the trends of the graph are assumed to be valid at high frequencies, then the extrapolated slope is the value of the modal density of the element at the higher frequencies.

6.4 STRUCTURAL COUPLING

The structural coupling parameter is unique to SEA. The definition of this parameter is one of more important steps in the SEA procedure. However, except for formulations describing the rigid connection of a few beam and plate situations, very little information is available on methods of calculating this parameter (or on this parameter in general). This lack of knowledge is mainly due to the relative newness of the SEA method. The

Table 4

MODAL DENSITIES OF SOME UNIFORM SYSTEMS*

System	Motion	Modal Density, $n(\omega)$**	Auxiliary Expressions
String	Lateral	$L/\pi c_S$	$c_s = \sqrt{T/\rho A}$
Shaft, Beam	Torsion	$L/\pi c_T$	$c_T = \sqrt{Gk/\rho J}$
Shaft, Beam	Longitudinal	$L/\pi c_\ell$	$c_\ell = \sqrt{E/\rho}$
Beam	Flexure	$\frac{L}{2\pi}\left(\omega \kappa_b c_\ell\right)^{-1/2}$	$\kappa_b c_\ell = \sqrt{EI/\rho A}$
Membrane	Lateral	$A_s\, \omega/2\pi c_m^2$	$c_m = \sqrt{S/\rho h}$
Plate	Flexure	$A_s/4\pi \kappa_p c_\ell$	$\kappa_p c_\ell = \sqrt{D/\rho h}$ $= \sqrt{Eh^2/12\rho(1-\nu^2)}$
Room, (Acoustic Volume)	Sound (Compression)	$V_o \omega^2/2\pi^2 c_a^3$	
Cylindrical Shells (Ref. 3)		$\begin{cases} \sim n_p & \text{for } \omega/\omega_r > 1 \\ \simeq n_p \left(\frac{\omega}{\omega_r}\right)^{2/3} & \text{for } \omega/\omega_r < 1 \end{cases}$	$\omega_r = c_\ell/a$ $np = A_s/4\pi\kappa_p c_\ell$
Doubly Curved Shells	Flexure	Expressions are complicated and not readily evaluated, see Ref. 4.	

*See next page for definitions of symbols.

**$N = \Delta\omega \cdot \eta(\omega)$

Symbol Definitions for Table 4

A	cross-section area
A_s	surface area
c_a	acoustic wave velocity
c_ℓ	Longitudinal wave velocity
c_m	membrane wave velocity
c_s	string wave velocity
c_T	torsional wave velocity
D	plate rigidity
E	Young's modulus
G	shear modulus
h	thickness
I	centroidal moment of inertia of A
J	polar moment of inertia of A
K	torsional constant of A
L	length
S	membrane tension force/unit edge length
T	string tension force
V_o	volume
κ_b	radius of gyration of A
κ_p	radius of gyration of plate cross section
ν	Poisson's ratio
ω	frequency (radians/time)
ρ	material density

equations for calculating the coupling of the various beam and plate joints are found in References 1, 6 and 7. Coupling relations for a few typical joints found in testing are also available in the literature.

When structural joints or energy paths (i.e. hard lines, bolted joints) unlike any previously defined in the literature are encountered, the value of the structural coupling must be empirically assigned to that joint. The known coupling parameters can sometimes be used as guidelines or upper bound solutions, but the reduction required for the approximate actual behavior of the structure is mainly a matter of judgement based on experience.

6.5 ACOUSTIC INPUT

The acoustic coupling representation used assumes that the external acoustic field is reverberant. The expression is of the form:

$$S = \frac{2\pi^2 \, C_0^2 \, A_i \, \langle \bar{p}^2 \rangle \, \sigma \, N_i}{\omega_0^2 \, (\Delta\omega) \, m_i}$$

If other acoustic fields are to be used as input, an "equivalent" reverberant field would need to be defined.

The radiation efficiency term, σ, may be approximated using procedures outlined in Reference 4, or may be determined from Figure 5.

6.6 MECHANICAL INPUT

A representation of mechanical input to the SEA model can be used when 1) the response of one element of the system is known, or 2) when the system is coupled to a known source of excitation.

In case 1, the known response of the element can be plugged directly into the system of equations. This reduces the order of the problem by one because it reduces the number of unknowns in the system of equations to be solved by one.

In case 2, the known external mechanical energy source is incorporated into the SEA model as another element. The system of equations is then handled as in case 1. Since the energy level of the source is known, the size of the problem is not affected by the addition of the mechanical source as another element. The system of equations can then be solved for the other element energy levels.

6.7 SEA RESPONSE PREDICTION EQUATIONS

The SEA response prediction equations consist of a set of equations that describe the energy state of element of the model. Each equation describes

1) the power into the element from an external source
2) the power dissipated within the element
3) the net power transferred between the element and any other element or elements coupled to it.

The general system of equations is of the form:

$$\begin{vmatrix} \alpha_{11} & \alpha_{12} & \cdots & \alpha_{1j} \\ & \alpha_{22} & \cdots & \alpha_{2j} \\ & & \ddots & \\ \text{SYMMETRIC} & & & \alpha_{ij} \end{vmatrix} \begin{Bmatrix} E_1 \\ E_2 \\ \vdots \\ E_i \end{Bmatrix} = \begin{Bmatrix} S_1 \\ S_2 \\ \vdots \\ S_i \end{Bmatrix}$$

$$\alpha_{ij} \begin{cases} -N_i \phi_{ij} & i \neq j \\ \omega \eta_j + \left(\sum_{k=1}^{6} N_k \phi_{ik} \right) & i = j \end{cases}$$

N_i = number of modes resonant in element i

η_i = element i loss factor

ϕ_{ij} = power transfer coefficient for coupling between modes in elements i and j (symmetric $\phi_{ij} = \phi_{ji}$)

ω = center frequency of the bandwidth

$E_i = m_i \frac{\overline{\langle a_i^2 \rangle}}{\omega^2}$ = total energy of element i

S_i = external acoustic or mechanical excitation in the bandwidth of interest

The unknowns of the set of equations are the total energy E_i at the average frequency ω. The system of equations are solved simultaneously for the unknown energy levels.

A two-element system can be used to see how these equations are divided.

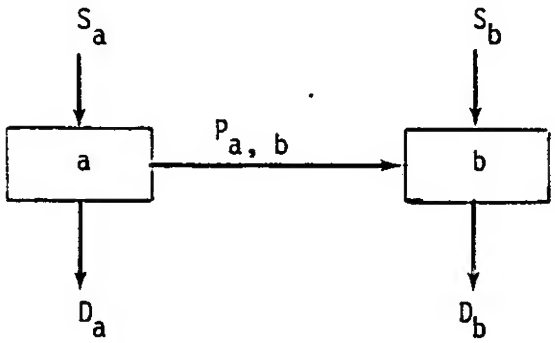

S_a = power introduced into element a from an external source in the bandwidth of interest.

D_a = power dissipated within element a in the bandwidth of interest.

$P_{a,\,b}$ = net power transmitted from element a to element b ($= -P_{b,\,a}$) in the bandwidth of interest.

The energy passing through the two elements in a single bandwidth can be expressed as:

$$D_a + P_{a,b} = S_a$$

$$D_b + P_{b,a} = S_b$$

To calculate solutions over the spectrum of interest, the system of equations is solved for each contributing frequency band.

The energy dissipated per unit time is defined in terms of the element loss factor as

$$D_a = \omega \eta_a E_a$$

where

ω = angular frequency (average) of system

η_a = element a loss factor

E_a = total energy of element a

The net power transmitted from the resonant modes of element a to the resonant modes of element b is

$$P_{a,b} = N_b \phi_{a,b} E_a - N_a \phi_{a,b} E_b$$

= (power transmitted from b to a) - (power transmitted from a to b)

where

N_a = number of modes resonant in element a

$\phi a,b$ = power transfer coefficient for coupling between modes through the structural joint ($\phi_{a,b} = \phi_{b,a}$)

Performing the indicated substitutions,

$$\omega \eta_a E_a + N_b \phi_{a,b} E_a - N_a \phi_{a,b} E_b = S_a$$

$$\omega \eta_b E_b + N_a \phi_{a,b} E_b - N_b \phi_{a,b} E_a = S_b$$

Regrouping the terms of the equation the general form of the response solution for two elements is obtained.

$$\begin{vmatrix} (\omega\eta_a + N_b\ \phi_{ab}) & -N_a\ \phi_{ab} \\ -N_b\ \phi_{ba} & (\omega\eta_b + N_a\ \phi_{ba}) \end{vmatrix} \quad \begin{Bmatrix} E_a \\ E_b \end{Bmatrix} = \begin{Bmatrix} S_a \\ S_b \end{Bmatrix}$$

η, N, ϕ and S are defined parameters, and the set of linear simultaneous equations can be solved for the unknowns E_a and E_b at the average frequency ω.

Section 7
REFERENCES

1. L. L. Beranek. Noise and Vibration Control. McGraw Hill Book Company, 1971.

2. R. W. Sevy and D. A. Earls. The Prediction of Internal Vibration Levels of Flight Vehicle Equipment Using Statistical Energy Methods. Technical Report AFFDL-TR-69-54, Air Force Flight Dynamics Laboratory, January 1970.

3. R. F. Davis. Statistical Energy Analysis Response Prediction Methods for Structural Systems - Final Report. McDonnell Douglas Astronautics Company Report MDC G8150, October 1979.

4. V. V. Bolotin. On the Density of the Distribution of Natural Frequencies of Thin Elastic Shells. J. Appl. Math. and Mech., Vol. 27, No. 2, 1963, pp 538-543.

5. D. N. Roudebush. Design Development Acoustic Fatigue Test of S-1VB/V Structural Aft Interstage Panels. Douglas Report SM-47320, Douglas Missile and Space Systems Division, 15 April 1966.

6. Richard H. Lyon. Statistical Energy Analysis for Designers. Technical Report AFFDL-TR-74-56, Part 1 and Part 2, Air Force Flight Dynamics Laboratory, January 1970.

7. R. H. Lyon and E. Eichler. Random Vibration of Connected Structures. J. Acoust. Soc. Am. Vol. 36, No. 7, July 1964, pp 1344-1354.

8. R. H. Lyon and G. Maidanik. Statistical Methods in Vibration Analysis. AIAA Journal, Vol. 2, No. 6, June 1964, pp 1015-1024.

END

DATE

FILMED

NOV 28 1980